Politecnico di Torino

Department of Electronics and Telecommunications

Characterisation of capacitive front-ends for indoor person localization

Master's Degree Thesis

Supervisor:
prof. Mihai Teodor LAZARESCU

Author:
Pellegrino D'Angelillo

Second reader:
prof. Luciano LAVAGNO

October 2020

Acknowledgements

Before leaving room for discussion, let me thank those who have supported me in my research. First of all, therefore, it is necessary to mention the supervisor of this thesis, Professor Mihai, who gave me valuable indications and corrections without which this work could not have seen the light of day. I would also like to thank the co-rapporteur, Professor Lavagno, who helped me to give a more concrete direction to the various research paths. They have transmitted to me that passion for research which is the source of true knowledge and improvement of ourselves before the world itself.

Outside of university, I have also found support and help from my entire family, and in particular from my father and mother, who have never made me lack their support throughout my studies, especially in times of great emotional and psychological difficulty.

Thanks to my brother with whom I have shared all my anxieties and doubts during these past years and to my little sister for all the love she transmitted to me.

Many thanks to my grandparents, always attentive and anxious about my university career, and to my uncle Franco for the good he has always shown me.

Finally, a thought I must reserve for all my classmates and friends, who have given me advice and encouragement throughout my university career.

In Loving Memory of Lorenzo

Abstract

Sensors for locating and identifying people indoors are currently extensively designed to monitor and automate systems. In the field of home automation, location sensors have become a key factor. There are different types of sensors that differ in their distinctive features: data processing, ease of installation, ease of use, privacy management: the latter is really important due to scalpers of the data of users in modern society. For these reasons, a localization system should have some particular features, such as being tagless, secure the user's privacy, and passive. In fact, some existing localization systems require people to wear or carry a tag to be monitored.

The most commonly used location sensors are radio frequency, infrared, pressure, ultrasound, video, and capacitive sensors. Capacitive sensors are here the subject of study because they have many advantages including good sensitivity compared to their size, are tagless and therefore suitable for any user, and protect the user privacy.

The project involves several areas of research, from the optimization of front-ends to the use of neural networks for location and identification algorithms.

During this thesis work on capacitive sensors, I worked with three different front-ends. My project focuses on the characterization of this three front-ends: a period modulator based on an RC astable oscillator circuit (RC-FE), another one, still period modulator, based on constant current charge-discharge (IC-FE) and a last one based on the ramp slope modulation (S-FE). All front-ends are based on the capacitive coupling between a metal plate and the human body: the resulting capacitance depends on the distance. Therefore, this capacitance is used, in the NE555 integrated circuit, to swing the RC-FE in astable mode with fixed resistance values whereas for IC-FE, oscillation is due to a Schmitt trigger that compares the capacitance voltage with the thresholds. These two front-ends return a square waveform at the output: in conclusion, the output period (frequency) of this circuits is measured. In the circuit S-FE based on slope modulation, the output value returns a triangular waveform, then the slope of the ramp is measured at the output instead of the oscillation period.

The three front-ends differ in the principle of operation and therefore in the circuit implementation. A very significant quantity for which they differ and on which a lot of attention will be paid is above all the output waveform of the three circuits. In fact, as mentioned above, if the RC-FE and IC-FE at the output present a square waveform of which you can measure

the period, the S-FE circuit instead presents a different waveform at the output, triangular, of which you can measure the slopes of the ramps and reach different conclusions in terms of the sensitivity parameter for example with respect to environmental noise.

The main objective of my thesis was to evaluate the measurement sensitivity. The sensitivities of interest are two: the sensitivity as a variation of the output signal (period or slope depending on the front-end) for small variations in the capacity of the armature and the sensitivity as a variation of the same output signal of the circuits (or similarly the capacity of the measured armature) compared to the variations of the noise component (environmental noise properly modelled).

For the front-ends I did simulations to evaluate different sensitivities but first and foremost an analytical calculation was used to support the results for the three front-ends: I have obtained the analytical formulas for all types of analysis simulated and analyzed their trend. In particular, my work has focused on analysis of the drift of the output value and of the plate capacitance calculation due to noise component.

The main tools used were Matlab as an environment for numerical calculations and LTspice [3] for circuit simulations.

With regard to the sensitivity of the capacitance calculation as measured capacitance changes in relation to changes in the noise component, it has been seen that the error introduced by the noise on the measurement (of the capacity) is almost constant with the frequency for RC-FE, while it decreases with the lowering of the noise frequency for IC-FE and S-FE and is much lower for the last one. Regarding the sensitivity values of the output of the front-ends for the different frequencies compared (sensitivity intended as a variation of the output signal compared to the same variations of the noise component), it has been seen that the sensitivity to changes in noise amplitude does not change with frequency: meaning that the variation in sensitivity to noise amplitude variations is really very small with frequency because there is a slight oscillation in the results, but this phenomenon is probably due to measurement errors.

Therefore, after data evaluations I found a very significant noise rejection of the circuit based on ramp slope modulation (S-FE) compared to the RC-FE circuit based on period modulator and quite significant compared to the circuit based on constant current period modulator (IC-FE). The results are significant since the very slow ambient noise turns out to invalidate the results obtained by the capacitive sensor: in fact these capacitive sensors could work for several hours.

It has been concluded that the three front-ends have different characteristics in terms of sensitivity both as a variation of the output signal for small variations of the armature capacity, and above all in terms of sensitivity as variations of the output signal or similarly of the measured capacity in relation to the variations of the noise component on which I have focused more.

Therefore, these significant results regarding the study and characterisation of these three front-ends can be taken as the reference point for subsequent research work and in particular starting from these results in order to be able to choose one front-end rather than another by virtue of its sensitivity values studied and validated both with simulations and analytically in this treatment. For example, S-FE can be chosen because of its higher rejection to long environmental noise rather than IC-FE or RC-FE, perhaps losing in terms of sensitivity with respect to small variations in the output signal or in other words the precision with which it is possible to locate a subject.

This and many other considerations can be made at the beginning of the next research work and on the basis of my results it will be possible to discern the most suitable front-end to start another experimental work.

In the future, we could investigate the use of a new front-end to lower the sensitivity value even more compared to the noise component.

Contents

List of Figures

List of Tables

1 Introduction

These days the localization and identification of people is a very significant topic, especially in the field of home automation, not only for safety reasons but also for environmental sustainability, such as lighting and heating in an increasingly "smart" home. It must be borne in mind that some of these monitoring systems may be pervasive in the sense that in order to work they may require the user to wear a certain type of equipment: for this reason it is essential to advance sensor-based location systems without tags which means that the sensor is able to locate people without them having to wear associated devices [8].

As already mentioned, there are two fundamental aspects that the system should have: one is to respect people's privacy and the other is to be ideally passive in such a way that it does not require in-depth knowledge and specific interactions. Therefore, this localization device must be absolutely transparent to the end user[2].

Another concern, that is the focus of this thesis work is the it is the problem of environmental noise that can affect the measurements of the output characteristics of the capacitive front-end, in particular the one with very long periods, and thus make the data to be processed for the subsequent phases of processing via neural networks, unusable.

1.1 Indoor human localization

There are many types of localization sensors based on different technologies and they have advantages and disadvantages.

- *Radiofrequency*: the human body absorbs radio signals: therefore sending a signal and receiving the return intensity of the same signal this gives not only indications about the position of people but also about their movements[16]. The radio frequency method is precise but the difficulty is to manage a necessary initial installation phase, which depends on the surrounding environment.

- *Pyroelectric sensors* [8]: they are inexpensive sensors but require a high computational effort. This type can provide additional information but have a small detection range. Two very important things are that they can be very easily subjected to to errors (heat/light sources) and may also be perplexing with regard to the issue of privacy [2].

- *Pressure sensor cells* [8]: they are reliable to identify people because of their almost unique weight, but they need to be installed under the floor, so its management is under discussion but they are transparent to users and are quite widespread [6].

- *Ultrasound sensors*, as treated in [8]: thanks to the wavelength (note), they can calculate the exact position of a person: they are such precise sensors but at the same time quite expensive. In addition, the individual device can cover just a limited amount of space. Two not insignificant disadvantages affect hearing, as far as humans are concerned, causing damage, and as far as pets are concerned, causing great annoyance and possible damage.

- Techniques with *cameras* and *Infrared thermal cameras*: require a very large computational effort, cost a lot and are not suitable for privacy nor for energy optimisation: all of which are not insignificant drawbacks, but which must be strictly taken into account.

- Techniques based on *RFID* , *Bluetooth* and *Wi-Fi* suffer interference but the biggest disadvantage is that users have to wear a tag, without which (they could easily forget) they would render the localization equipment unusable.

The following work concentrates on *capacitive sensors*, which are quite suitable for detection and monitoring, are tag-free, economical, work in respect of privacy and can be not only optimized for low power consumption [1] but also to reject noise with a long period.

The wider research project aims to optimize the capacitive detection in terms of noise rejection, power optimization, accuracy and flow rate increase. In the field of capacitive sensing, several really interesting explorations have led to the *movement sensor* Electric potential sensor (EPS) as reported especially in [12]. This typology works for long distances (several meters) using the slow variation of environmental electric fields but is very susceptible to noise. In [15] this sensor was also used to detect a human being's breath at a distance of three feet. It is also difficult to quickly reveal people's movements.

Our team at the Polytechnic of Turin work on the development, optimization and research on capacitive detection. This thesis is part of this much larger project focusing on noise rather than environmental noise over long periods of time that affects the capacitive front-end and in particular the output characteristic of the latter.

1.2 Capacitive sensing

Capacitive sensing, mentioned among the above mentioned techniques, is widely used: the touch of almost all mobile phones and those of some laptops. It is a technique that allows to perceive the proximity or a touch as an ability. Therefore it is a moderately simple technique as it is easy to measure a capacitance value. So the capacitance is converted into a measurement of frequency or slope of a ramp depending on the front-end used and we will develop an in-depth discussion for each of the three front-ends analyzed in this thesis work in the next dedicated sections. As regards the more general discourse of capacitive coupling, the human body is a conductive element that couples with the environment, therefore these sensors can be used to track a person's position relative to them.

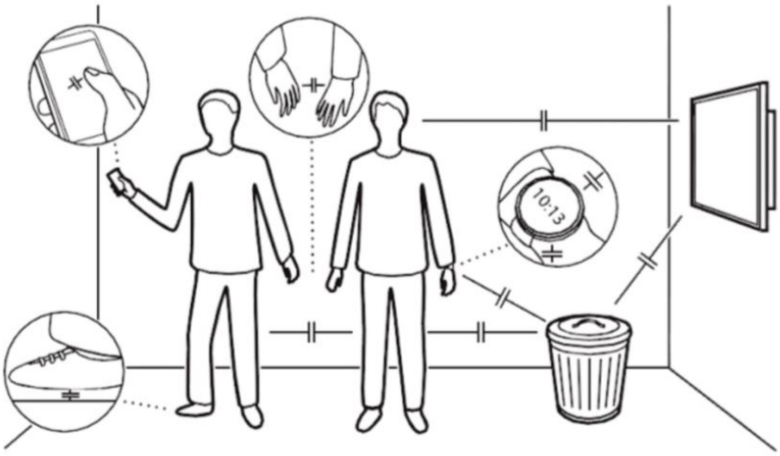

Figure 1: Capacitive coupling between human body and the environment

As shown in the Figure 1 and with reference to [5]the human body produces capacitances with all the objects surrounding it (including another body which is also conductive): the human body behaves as a single conductive plate of the ideal parallel plane face capacitor, with air as dielectric, with air as dielectric. The common ground is a potential shared by the two plates (floor potential, body itself).

From the theory it is known that there is a capacitance where there are two different conductive elements separated by a dielectric and that there is also an electric field if the latter are at different potentials. The CAPACITANCE **C** is the CHARGE **Q** held by the capacitor divided by the VOLTAGE **V**:

$$C = \frac{Q}{V} \tag{1}$$

The capacitance for a planar capacitor, cited in [13], depends on the AREA of the two faces **A**, the DISTANCE between them **d** (bearing in mind that A $\gg$ d) according to the following relation in which the absolute dielectric constant permectivity of free space ϵ_0 (8.854×10^{-12} F/m) and the relative dielectric permittivity of the material between the plates (k = 1 in case of free space) **k** appear :

$$C = \frac{\epsilon_0 k A}{d} \tag{2}$$

For the sensor there is still a dependency between the capacitance and the distance from the plate, but the relationship between these two sizes is not the one mentioned above but an approximate formula is:

$$C \sim \frac{k \cdot A}{d^{2-3}} \tag{3}$$

The Figure below 2 taken from [6] shows the capacitive coupling between the sensor, the objects around it and the human body.

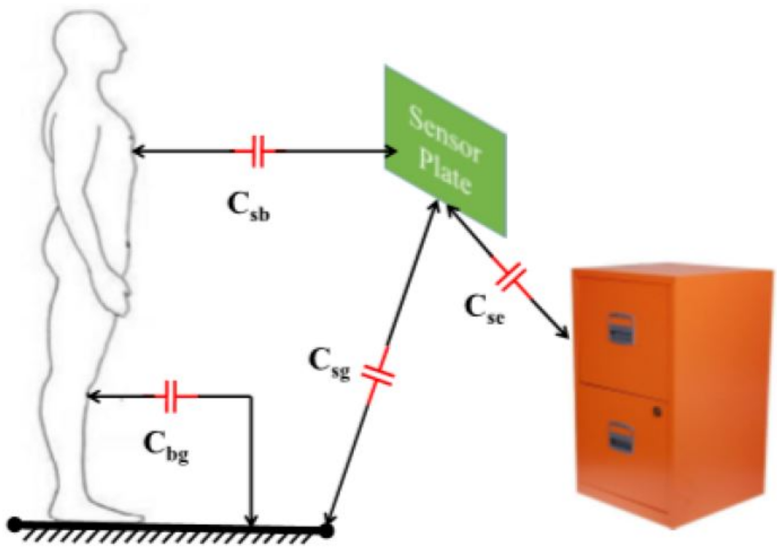

Figure 2: Capacitive coupling between sensor, objects and human body

The main capacitance components are:

- C_{sb}, between human body and the sensor plate
- C_{bg}, between human body and ground floor
- C_{sg}, between the sensor plate and ground floor
- C_{se}, between the sensor plate and other objects in the environment

It must be taken into account that humidity and ambient temperature affect the air dielectric and these capacities. The C_{sb} is what we are interested in measuring and is a function of the distance between the sensor and the human body.

1.2.1 Working modes

There are mainly three working modes for capacitive sensing and are illustrated below:

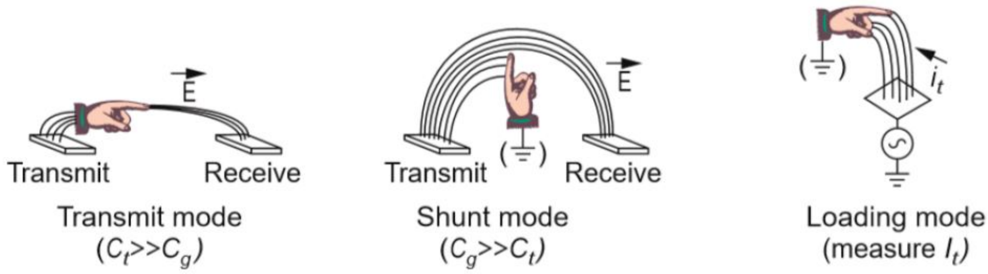

Figure 3: Different capacitive sensing modes

Looking at the three systems described in [14] and shown in Figure 3, you can see how two of them involve the use of one sensor for transmission and one for reception.

Going into more detail:

- *Transmit mode*: in this way the human body is part of the transmitter, so that the received signal is increased by a value that depends on the proximity of the body. Due to the prevalence of the capacitance between the body and plate compared to the body-ground capacitance, this is possible for a very close distance between the body and the transmitter. This would not be an easy and tag-less method.

- *Shunt mode*: the received signal is decreased with body proximity: the body is not very close to the plates and the body the land capacitance prevails. Like the transmit mode is a robust way to transfer a large amount of information.

- *Loading mode*: only one plate is needed (it is less complex): measure the induced current in the plate. Both the body and the plate are indicated at a shared earth potential [14].

1.3 Previous research

The thesis works preceding mine (as for example some of them are [13] [4] [2] [11] [9]) investigate different aspects from the development to the optimization of the different front-ends for the localization of the human being in closed environments and not only.

This research work has been carried on over time and continued (as I am doing in this thesis) improving some aspects and finding new ones for the development of new front-ends capable of optimizing some features of the system or being less subject to environmental noise and so on.

The researchers of the team have made some experiences in sensor laboratories but also simulating on simulation environments like LTspice [3] their behavior over time.

1.4 Project

The main objective of this thesis project is to analyze and characterize three different capacitive front-ends compared to the previous work in this research project.

In detail, my thesis focuses on the evaluation of the measurement sensitivity. The sensitivities of interest are two: the sensitivity as a variation of the output signal (period or slope depending on the front-end) for small variations in the capacity of the armature and the sensitivity as a variation of the same output signal of the circuits (or similarly the capacity of the measured armature) compared to the variations of the noise component (environmental noise properly modelled).

My project focuses on the characterization of this three front-ends: a period modulator based on an RC astable oscillator circuit (RC-FE), another one, still period modulator, based on constant current charge-discharge (IC-FE) and a last one based on the ramp slope modulation (S-FE). All front-ends are based on the capacitive coupling between a metal plate and the human body: the resulting capacitance depends on the distance. Therefore, this capacitance is used, in the NE555 integrated circuit, to swing the RC-FE in astable mode with fixed resistance values whereas for IC-FE, oscillation is due to a Schmitt trigger that compares the capacitance voltage with the thresholds. These two front-ends return a square waveform at the output: in conclusion, the output period (frequency) of this circuits is measured. In the circuit S-FE based on slope modulation, the output value returns a triangular waveform, then the slope of the ramp is measured at the output instead of the oscillation period.

For the front-ends I did simulations to evaluate different sensitivities but first and foremost an analytical calculation was used to support the results for the three front-ends: I have obtained the analytical formulas for all types of analysis simulated and analyzed their trend. In particular, my work has focused on analysis of the drift of the output value and of the plate capacitance calculation due to noise component.

The starting point has been the implementation of the three different front-ends, according to [13] and [10] schemes and arguments. Throughout the whole process, particular attention has been devoted to the scrupulous analysis of the different systems, preserving the correct functioning of the same and trying to characterize them at their best.

2 Capacitive sensor front-end based on RC period modulator (RC-FE)

2.1 Operating principle

In this subsection has been introduced the theory behind this sensor.The RC-FE based capacitive sensor is based on capacitive coupling between a metal plate and the human body. In fact, the human body couples with objects in the environment and the resulting capacitance depends on the distance. Therefore, this capacitance is used to oscillate the RC-FE in astable mode with fixed values of the resistances. Finally, the oscillation frequency of the output square wave is measured.

Looking in detail at the configuration of the RC-FE circuit has been used in stable mode, such as shown in Figure 4 taken from [13], with a metal plate that couples with the human body, two fixed resistors values. The RC-FE output presents a square wave whose characteristics depend on the resistance value and the capacitance value. The former have been fixed, so the frequency of the output signal depends only on the capacitance, which in turn depends on the distance between the plate and the human.

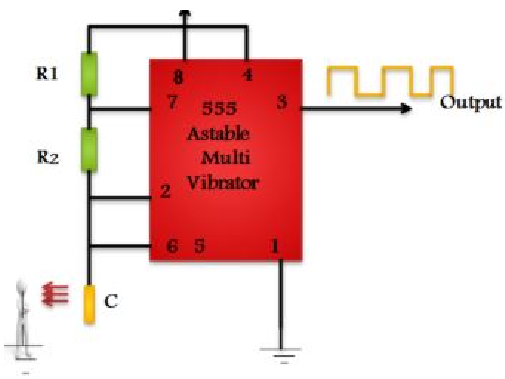

Figure 4: RC-FE high-level schematic

The expression that gives the frequency of the output signal to RC-FE is as follows:

$$f_{RC-FE} = \frac{k}{(R_1 + 2R_2) \cdot C} \tag{4}$$

with k = 1.44.

2.2 Implementation

For the capacitive sensor, that actually measures the distance of a person from it, the setup is based on a RC-FE used as astable oscillator: an idealized RC-FE timer model. The circuit has been simulated with LT-spice [3] under different detailed conditions and divided case by case in the following sections of this work. Subsequently, as already mentioned, the output waveform was analyzed and with the help of algorithms pulled out the characteristics of the latter by further processing these characteristics such as period and frequency which were used to indirectly calculate the capacitance of the plate.

The diagram of the analyzed RC-FE used as an oscillator can be seen in Figure 5 from [7]:

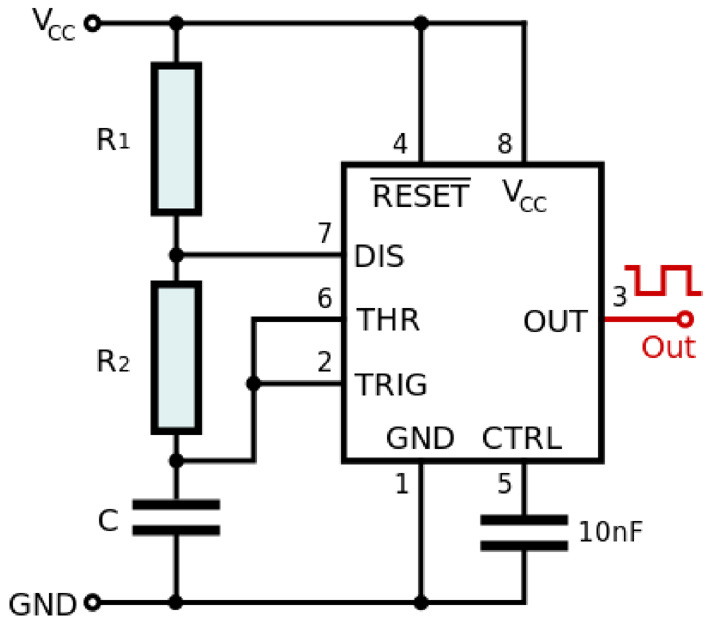

Figure 5: RC-FE schematic for astable mode

Below the simulation schematic of the circuit mentioned before in LTspice:

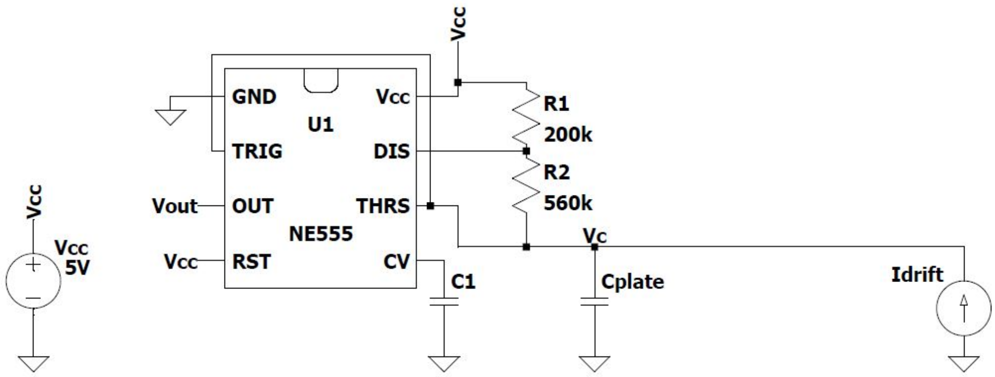

Figure 6: Schematic of the RC period modulator sensor

with $C_1 = 10$ nF.

Considerations

A disadvantage in the use of this type of front-end based on RC-FE is its low noise rejection.

3 Capacitive sensor front-end based on constant current period modulator (IC-FE)

3.1 Operating principle

The period modulation interface with the block diagram shown in Figure 7 takes from [10] cyclically charges and discharges the plate capacitance C_{plate} using a voltage-controlled current source with a constant current I:

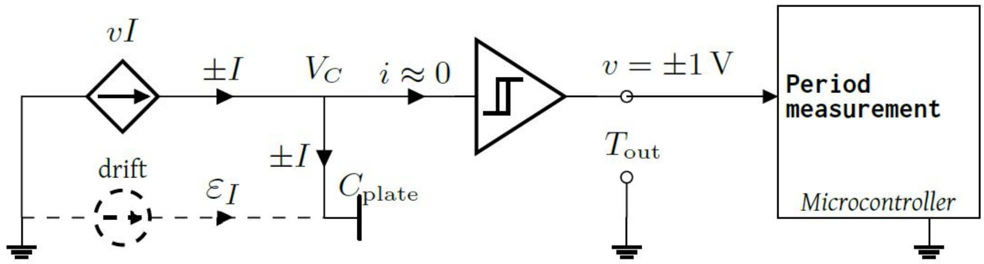

Figure 7: Period modulation interface circuit considering drift current ϵ_I

This source changes linearly the plate voltage V_C as shown by the dashed plot in Figure 8, shown below, from [10]:

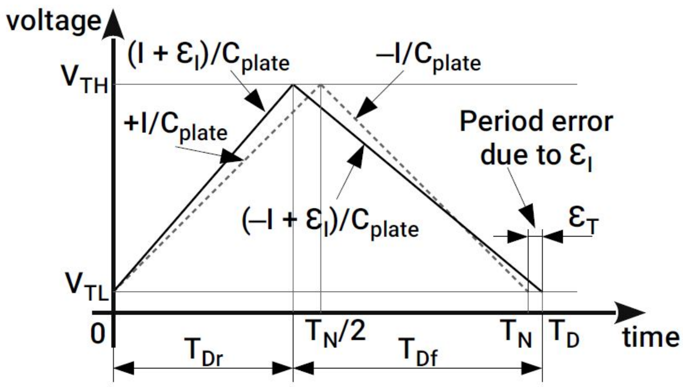

Figure 8: Period errors due to drift current ϵ_I from charge induction

Remember that the capacitance C of an object is by definition the division between its charge variation ΔQ and its potential variation ΔV_C:

$$C = \frac{\Delta Q}{\Delta V_C} \tag{5}$$

Therefore:

$$C_{\text{plate}} = \frac{I\Delta t}{\Delta V_C} \quad \text{or} \quad \Delta V_C = \frac{I}{C_{\text{plate}}}\Delta t \tag{6}$$

When V_C reaches the thresholds of a hysteresis IC-FE (V_{TL}, V_{TH}), its output v swings, changing the sign of I.

Assuming constant C_{plate} and no noise, the charge and discharge times are identical:

$$C_{\text{plate}} \frac{V_{\text{TH}} - V_{\text{TL}}}{I} = C_{\text{plate}} \frac{V_{\text{TL}} - V_{\text{TH}}}{-I} = \frac{T_{\text{N}}}{2} \tag{7}$$

with:

$$V_{TH} = V_{SAT} \cdot \frac{R_1}{R_2} \tag{8}$$

and

$$V_{TL} = -V_{SAT} \cdot \frac{R_1}{R_2} \tag{9}$$

using R_1 and R_2 that are referred to Fig.9.

In this way it is possible to trace the C_{plate} value by measuring the period of oscillation of the output IC-FE waveform In this way it is possible to trace the C_{plate} value by measuring the period of oscillation of the output IC-FE waveform:[10]:

$$C_{\text{plate}} = \frac{I}{2\left(V_{\text{TH}} - V_{\text{TL}}\right)} T_{\text{N}} \tag{10}$$

3.2 Implementation

In this subsection will be discussed the simulation schematic of the circuit mentioned before.

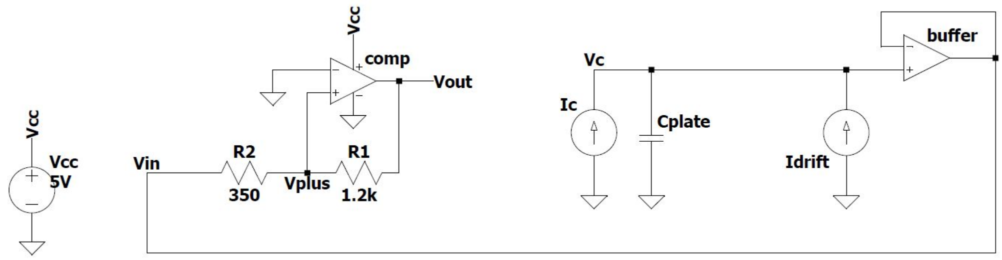

Figure 9: Schematic of the constant current astable multivibrator sensor

3.2.1 Sensor

The first block implemented is the sensor itself. Period modulation interfaces Fig. 9 repeatedly charge and discharge the plate capacitance C_{plate} using a voltage-controlled current source with a constant current I as stated above.

When V_C reaches the thresholds of a hysteresis IC-FE (V_{TL}, V_{TH}), its output v swings, changing the sign of I to satisfy $V_{TL} \leq V_C \leq V_{TH}$.

3.2.2 Drift Current

In the circuit there is also a "I_{drift}" current source, between the ground and the "V_C" node, which was necessary in the following to insert and model the noise. This will be discussed specifically later when moving on to sensitivity measurements.

3.2.3 Buffer

It is an amplifier that provides the impedance transformation, reducing the value, in the connections between circuits. It is used to transfer a voltage from a first circuit, at high impedance level, to a second circuit, at lower impedance level.

The interposed buffer prevents the second circuit from overloading the first circuit and altering its operation.

In this case the voltage is transferred unchanged, therefore, the buffer is a unitary gain amplifier: also known as a voltage tracker.

Its realization by means of an operational amplifier involves very simply returning the output signal of an operational amplifier to its inverting input (negative feedback), and applying the input signal to its non-inverting input.

This device is obtained by closing an operational amplifier in unitary feedback, i.e. by returning the output signal directly to the inverting input of the amplifier.

The main purpose of the buffer is to separate or decouple the signal source from the rest of the circuit. Decoupling allows the signal source not to draw current from the signal source, thus not causing load effects, i.e. excessive current absorption from the signal generator, and thus increasing the generator's ability to supply power.

3.2.4 Schmitt's non-inverting Trigger

At the end of the whole sensor, a threshold IC-FE is present. The Schmitt trigger is a particular type of threshold IC-FE with hysteresis, i.e. a circuit that allows to transform an analog signal into an output that varies only between two voltage values depending on whether the input exceeds a certain threshold or is lower than a second (lower) threshold.

The Schmitt trigger has an input voltage and an output voltage. The output can be either low or high. At the input the trigger has two thresholds, one high and one low not coincident: in a non-inverting circuit, like this one, when the input is below the low threshold, the output assumes the low value; when the input is above the high (highest) threshold, the output assumes the high value. When the input value is between the two thresholds, the output retains the previous value until the input has changed sufficiently to trigger the change (trigger action). This operation implies some memory in the trigger that is called hysteresis.

The advantage of Schmitt's trigger over other systems similar to a single input threshold is its greater stability: with a single input threshold, a noisy input signal, close to the threshold value, can oscillate rapidly around this value, making the output oscillate between its low and high value; with Schmitt's trigger, a noisy signal close to a threshold can cause a single switching of the output value, after which it must grow towards the other threshold in order to cause further switching.

Schmitt's Trigger is used here to make a simple type of relaxation oscillator or multivibrator of the astable type.

3.2.5 Complete circuit

The whole circuit provides a digital signal to the output with a certain output period value (in accordance with report 9) depending on the value of the capacitance of the dish only: since all other quantities are fixed (V_{TH} and V_{TL}).

4 Capacitive sensor front-end based on constant current slope modulator (S-FE)

In the previous work, another front-end has been developed, for human localization with capacitive sensor, the one presented in [10] and its schematic is reported in 10.

4.1 Operating principle

The operation of the slope modulation measurement interface in Fig. 10 shown below is similar to period modulation interface in Fig. 7.

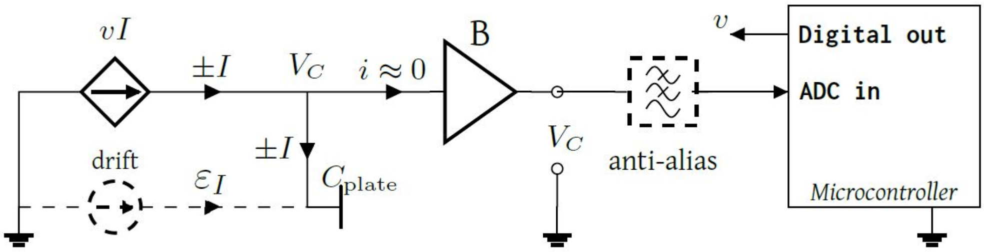

Figure 10: Capacitance-to-slope conversion circuit with drift current, ϵ_{I}

But here we keep the timing constant and independent of C_{plate}. From (6), V_{C} ramp slope S is inversely proportional to C_{plate}

$$S = \frac{\Delta V_C}{\Delta t} = \frac{I}{C_{\text{plate}}} \tag{11}$$

4.2 Implementation

In this subsection will be discussed the simulation schematic of the circuit mentioned before.

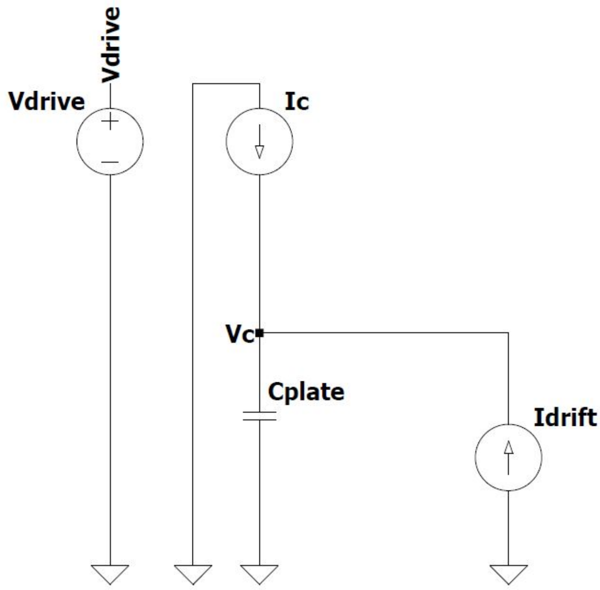

Figure 11: Schematic of the dual ramp sensor

4.2.1 Sensor

The first block implemented is always the sensor itself. Slope modulation interfaces Fig. 11 repeatedly charge and discharge the plate capacitance C_{plate} using a voltage-controlled current source with a constant current I .

4.2.2 Drift Current

In the circuit there is also a "I_{drift}" current source, between the ground and the "V_C" node, which was necessary in the following to insert and model the noise. This will be discussed specifically later when moving on to sensitivity measurements as repeatedly stated.

5 Brief front-end comparisons

The three front-ends differ in the principle of operation and therefore in the circuit implementation as widely discussed so far.

A very significant quantity for which they differ and on which a lot of attention will be paid is above all the output waveform of the three circuits. In fact if the RC-FE and IC-FE at the output present a square waveform of which you can measure the period, the S-FE circuit instead presents a different waveform at the output, triangular, of which you can measure the slopes of the ramps and reach different conclusions in terms of the sensitivity parameter for example with respect to environmental noise.

The sensitivities of interest and that will be deepened in the next sections are two: the sensitivity as a variation of the output signal (period or slope depending on the front-end) for small variations in the capacity of the armature and the sensitivity as a variation of the same output signal of the circuits (or similarly the capacity of the measured armature) compared to the variations of the noise component.

6 Analytical results

In this section we have obtained the analytical formulas for all types of analysis that we have simulated so far and analyzed their trend.

An analytical calculation was used to support the results for the three front-ends.

6.1 Front-end output sensitivities to input capacitance variations

RC-FE

- The expression that gives the frequency of the output signal for RC-FE is given by (4), the sensitivity of interface output frequency to C_{plate} changes is:

$$S_f = \frac{\partial f}{\partial C_{\mathrm{plate}}} = -\frac{1}{0.693\,(R_1 + 2R_2)} \cdot \frac{1}{C^2_{\mathrm{plate}}} \tag{12}$$

with:
C_{plate}= 60 pF;
R_1 = 200 $k\Omega$;
R_2 = 560 $k\Omega$.

IC-FE

- The expression that gives the frequency of the output signal for IC-FE is given by (10), the sensitivity of interface output frequency to C_{plate} changes is:

$$S_f = \frac{\partial f}{\partial C_{\mathrm{plate}}} = -\frac{1}{2\,(V_{\mathrm{TH}} - V_{\mathrm{TL}})} \cdot \frac{I}{C^2_{\mathrm{plate}}} \tag{13}$$

with:
C_{plate}= 6 pF;
V_{TH} = 0.7292 V;
V_{TL} = -0.7292 V;
and:
I = 27 nA.

S-FE

- The expression that gives the slope of the output signal for S-FE is given by (11), the sensitivity of interface output slope to C_{plate} changes is:

$$S_S = \frac{\partial S}{\partial C_{\text{plate}}} = -\frac{I}{C_{\text{plate}}^2} \tag{14}$$

with:
C_{plate}= 25 pF;
I = 112.5 nA.

This output sensitivity to C_{plate} variations is comparable with that of the period modulation interface in (13)

In Table 1 the analytical calculation of the sensitivity values:

	RC-FE	IC-FE	S-FE
Output sensitivity	1.00777	0.95967	1.00000

Table 1: Absolute value of front-end output sensitivities to capacitance variations calculated analytically with relative difference

In Fig.12 the analytical results graphically.

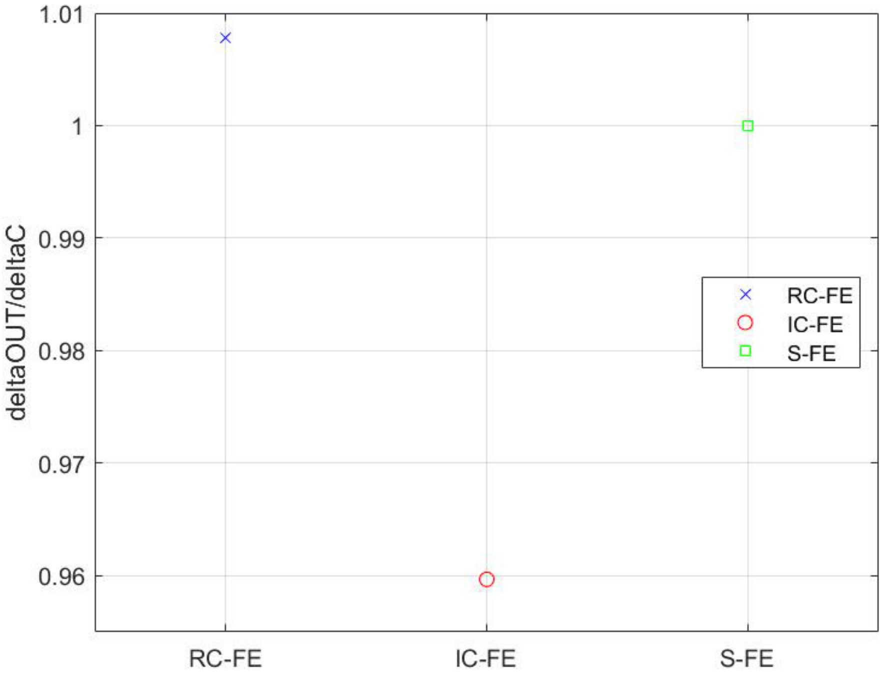

Figure 12: Analytical results of front-end output sensitivities to input capacitance variations

In Table 2 results of output sensitivities were obtained with the analytical calculation around nominal capacity values: nominal capacity of RC-FE is 60pF,for IC-FE is 6pF and for S-FE is 25pF.

capacity values around nominal	RC-FE	IC-FE	S-FE
+1%	0.98791	0.94076	0.98029
-1%	1.02823	0.97916	1.02030
+5%	0.91407	0.87045	0.90703
-5%	1.11664	1.06335	1.10803
+10%	0.83287	0.79312	0.82644
-10%	1.24416	1.18478	1.23457

Table 2: Absolute value of front-ends output sensitivities to capacitance variations calculated analytically with capacity values around nominal

6.2 Front-end sensitivity to noise amplitude

6.2.1 Errors due to constant noise current (DC)

RC-FE

- From current–voltage relation for capacitances, where the intensity of a current i(t) varies over time, we know that

$$C_{\text{plate}} = \frac{\int i(t)\,dt}{\Delta V_C} \tag{15}$$

while the equation of current as a function of time for a RC circuit is written as

$$i(t) = \frac{V_0}{R} e^{-t/(RC)} \tag{16}$$

where V_0 is the constant potential difference at the ends of C_{plate}.

Therefore assuming constant C_{plate} and no noise for the moment, the charge time for RC-FE, w.r.t. Fig.13, is:

$$T_{Dr} = C_{\text{plate}} \frac{V_{\text{TH}} - V_{\text{TL}}}{\int_0^{t_1} i_c(t)\,dt} \tag{17}$$

while the discharge time for RC-FE, w.r.t. Fig.13, is:

$$T_{Df} = C_{\text{plate}} \frac{V_{\text{TL}} - V_{\text{TH}}}{\int_{t_1}^{t_2} -i_d(t)\,dt} \tag{18}$$

where the the charging and discharging currents of the capacitor are variable (RC) (Fig. 13) and respectively equal to

$$i_c(t) = \frac{V_{cc}}{(R_1 + R_2)} \cdot e^{-\frac{t}{(R_1+R_2)\cdot C_{plate}}} \tag{19}$$

$$i_d(t) = \frac{V_{TH}}{R_2} \cdot e^{-\frac{t}{R_2 \cdot C_{plate}}} \tag{20}$$

because the circuit RC-FE by 555 IC charges the capacitance through R_1 and R_2 resistors and discharges it only with the R_2 resistor.

The times of high output pulse and of low output pulse (Fig. 13) are respectively equal to

$$t_1 = k\,(R_1 + R_2) \cdot C_{plate} \tag{21}$$

$$t_2 = k \cdot R_2 \cdot C_{plate} \tag{22}$$

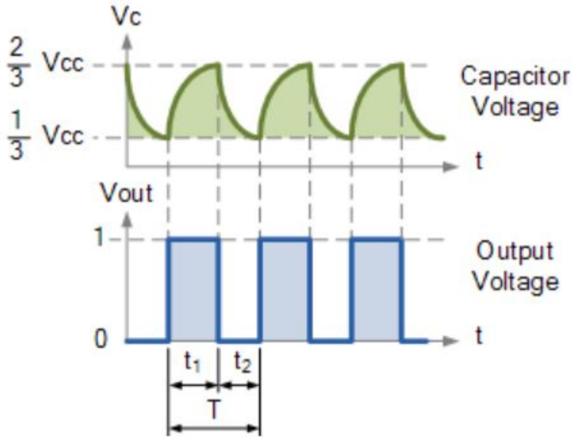

Figure 13: Diagram for reference to significant quantities (RC-FE)

and the calculation of the two integrals as follows:

$$\int_0^{t_1} i_c(t)dt = \int_0^{t_1} \frac{V_{cc}}{(R_1+R_2)} \cdot e^{-\frac{t}{(R_1+R_2)\cdot C_{plate}}} dt = \frac{V_{cc}}{(R_1+R_2)} \cdot \int_0^{t_1} e^{-\frac{t}{(R_1+R_2)\cdot C_{plate}}} dt =$$
$$= -(R_1+R_2) \cdot C_{plate} \cdot e^{-k} + (R_1+R_2) \cdot C_{plate} = (R_1+R_2) \cdot C_{plate} \cdot \left(-e^{-k}+1\right)$$

and

$$\int_{t_1}^{t_2} -i_d(t)dt = \int_{t_1}^{t_2} -\frac{V_{TH}}{R_2} \cdot e^{-\frac{t}{R_2 \cdot C_{plate}}} dt = -\frac{V_{TH}}{R_2} \cdot \int_{t_1}^{t_2} e^{-\frac{t}{R_2 \cdot C_{plate}}} dt =$$
$$= R_2 \cdot C_{plate} \cdot e^{-k} - R_2 \cdot C_{plate} \cdot e^{-\frac{k(R_1+R_2)}{R_2}} = R_2 \cdot C_{plate} \cdot \left(-e^{-k} + e^{-\frac{k(R_1+R_2)}{R_2}}\right)$$

with:
$V_{\mathrm{cc}} = 5$ V;
k = 0.7 (specific constant for circuit thresholds 555);
$V_{\mathrm{TH}} = \frac{2}{3} \cdot V_{cc}$ and $V_{\mathrm{TL}} = \frac{1}{3} \cdot V_{cc}$ (Fig. 13).

However, a quasi-constant drift noise current ε_I is superimposed and for the noise superposition theorem on the charge-discharge of an RC circuit, the rising T_{Dr} and falling T_{Df} ramp durations in (17) and (18) change

$$T_{\mathrm{Dr}} = C_{\mathrm{plate}} \frac{V_{\mathrm{TH}} - V_{\mathrm{TL}}}{[(R_1 + R_2) \cdot C_{plate} \cdot (-e^{-k} + 1)] + \varepsilon_I} \tag{23}$$

$$T_{\mathrm{Df}} = C_{\mathrm{plate}} \frac{V_{\mathrm{TL}} - V_{\mathrm{TH}}}{[R_2 \cdot C_{plate} \cdot (-e^{-k} + e^{-\frac{k(R_1+R_2)}{R_2}})] + \varepsilon_I} \tag{24}$$

and oscillation period T_D of the measurement interface becomes

$$T_{\mathrm{D}} = T_{\mathrm{Dr}} + T_{\mathrm{Df}} \tag{25}$$

From

$$\mathrm{T} = k\,(\mathrm{R}_1 + 2 \cdot \mathrm{R}_2) \cdot \mathrm{C}_{\mathrm{plate}}$$

and (25) we can calculate the relative measurement error (period):

$$T_r = \frac{T_{\mathrm{D}} - T}{T} \tag{26}$$

with:
k = 0.7;
$\varepsilon_I = 50$ nA;
$R_1 = 200\ k\Omega$;
$R_2 = 560\ k\Omega$;
$C_{plate} = 60$ pF.
$V_{TH} = \frac{10}{3}$ and $V_{TL} = \frac{5}{3}$;

Table 3 the relative measurement error (period) for RC-FE:

capacity value	T_r for RC-FE
60pF	4.085948

Table 3: Relative measurement error (period) for RC-FE

In Table 4 results of the relative measurement error (period) were obtained with the analytical calculation around nominal capacity values for RC-FE: nominal capacity of RC-FE is 60pF.

capacity values around nominal	T_r for RC-FE
+1%	0.40787
-1%	0.39578
+5%	0.43067
-5%	0.37005
+10%	0.45680
-10%	0.33463

Table 4: Relative measurement error (period) for RC-FE with capacity values around nominal(60pF)

IC-FE

From Article [10] has taken the expression of the relative measurement error of the period obtained as follows:

- Considering the charge-discharge current I constant, from current–voltage relation for capacitances we know that:

$$C_{\text{plate}} = \frac{I\Delta t}{\Delta V_C} \quad \text{or} \quad \Delta V_C = \frac{I}{C_{\text{plate}}}\Delta t \tag{27}$$

  Therefore assuming constant C_{plate} and no noise, the charge and discharge times are identical:

$$C_{\text{plate}}\frac{V_{\text{TH}} - V_{\text{TL}}}{I} = C_{\text{plate}}\frac{V_{\text{TL}} - V_{\text{TH}}}{-I} = \frac{T_{\text{N}}}{2} \tag{28}$$

  However, a quasi-constant drift current ε_I unbalances the rising T_{Dr} and falling T_{Df} ramp durations in (28)

$$T_{\text{Dr}} = C_{\text{plate}}\frac{V_{\text{TH}} - V_{\text{TL}}}{I + \varepsilon_I}, \quad T_{\text{Df}} = C_{\text{plate}}\frac{V_{\text{TL}} - V_{\text{TH}}}{-I + \varepsilon_I} \tag{29}$$

  and oscillation period T_D of the measurement interface becomes

$$T_{\text{D}} = T_{\text{Dr}} + T_{\text{Df}} = \frac{2C_{\text{plate}}\left(V_{\text{TH}} - V_{\text{TL}}\right)I}{I^2 - \varepsilon_I^2} \tag{30}$$

  From (28) and (30) we can calculate the relative measurement error (period):

$$T_r = \frac{T_{\text{D}} - T_{\text{N}}}{T_{\text{N}}} = \frac{I^2}{I^2 - \varepsilon_I^2} - 1 = \frac{\varepsilon_I^2}{I^2 - \varepsilon_I^2} \tag{31}$$

  with the parameters T_D and T_N that refer to the Figure 8 and with:
  I = ± 27 nA;
  $\varepsilon_I = 0.0027$ nA.

Table 5 the maximum and minimum relative measurement error (period) for IC-FE:

IC-FE	Maximum	Minimum
T_r	$0.01x10^{-6}$	$-0.009x10^{-6}$

Table 5: Maximum and minimum relative measurement error (period) for IC-FE

S-FE

From [10] has taken the expression of the relative measurement error of the slope, whose derivation calculations are given below:

- From (27), ramp slope S is inversely proportional to Cplate:

$$S = \frac{\Delta V_C}{\Delta t} = \frac{I}{C_{\text{plate}}} \tag{32}$$

A constant drift current ε_I changes rising S_r and falling S_f slopes

$$S_r = \frac{I + \varepsilon_I}{C_{\text{plate}}}, \quad S_f = \frac{-I + \varepsilon_I}{C_{\text{plate}}} \tag{33}$$

but we notice that slope magnitude average S_a is invariant to ε_I

$$S_a = \frac{|S_r| + |S_f|}{2} = \frac{1}{2}\left(\frac{I + \varepsilon_I}{C_{\text{plate}}} - \frac{-I + \varepsilon_I}{C_{\text{plate}}}\right) = \frac{I}{C_{\text{plate}}} \tag{34}$$

with:
I = ± 112.5 nA;
ε_I = 1.125 nA;
C_{plate} = 25 pF.

Table 6 the maximum and minimum slope magnitude average S_a for S-FE:

IC-FE	Maximum	Minimum
S_a	4500	-4500

Table 6: Maximum and minimum slope magnitude average S_a for S-FE

In Table 7 results of the maximum and minimum slope magnitude average S_a for S-FE were obtained with the analytical calculation around nominal capacity values for S-FE: nominal capacity of S-FE is 25pF.

capacity values around nominal	Maximum S_a for S-FE	Minimum S_a for S-FE
$+1\%$	4455	-4455
-1%	4545	-4545
$+5\%$	4285	-4285
-5%	4736	-4736
$+10\%$	4090	-4090
-10%	5000	-5000

Table 7: Maximum and minimum slope magnitude average S_a for S-FE with capacity values around nominal(25pF)

Hence, using (34) we can calculate C_{plate} rejecting quasi-constant drift currents ε_I as common mode signals by measuring the slope of two adjacent charge-discharge ramps, as highlighted in the Article [10].

6.2.2 Errors due to linearly varying noise current (ramp)

First of all, we define the general model of the noise current that varies linearly over time that will be used later in the discussion and it is the following:

$$I_n(t) = R_{n0} + \varepsilon_n \cdot t \tag{35}$$

RC-FE

- here the overlapping current varies linearly and once again this one changes the rising T_{Dr} and falling T_{Df} ramp durations in (17) and (18)

$$T_{\mathrm{Dr}} = C_{\mathrm{plate}} \frac{V_{\mathrm{TH}} - V_{\mathrm{TL}}}{[(R_1 + R_2) \cdot C_{plate} \cdot (-e^{-k} + 1)] + (\varepsilon_I \cdot t)} \tag{36}$$

$$T_{\mathrm{Df}} = C_{\mathrm{plate}} \frac{V_{\mathrm{TL}} - V_{\mathrm{TH}}}{[R_2 \cdot C_{plate} \cdot (-e^{-k} + e^{-\frac{k(R_1+R_2)}{R_2}})] + (\varepsilon_I \cdot t)} \tag{37}$$

and oscillation period T_D of the measurement interface becomes

$$T_{\mathrm{D}} = T_{\mathrm{Dr}} + T_{\mathrm{Df}} \tag{38}$$

From

$$\mathrm{T} = k\,(\mathrm{R}_1 + 2 \cdot \mathrm{R}_2) \cdot \mathrm{C}_{\mathrm{plate}}$$

and (38) we can calculate the relative measurement error (period):

$$T_r = \frac{T_{\mathrm{D}} - T}{T} \tag{39}$$

IC-FE

In this case the overlapping noise current is not quasi-constant current but it varies linearly, so (29) changes.

- In fact a noise current that varies linearly unbalances the rising T_{Dr} and falling T_{Df} ramp durations in (28)

$$T_{\mathrm{Dr}} = C_{\mathrm{plate}} \frac{V_{\mathrm{TH}} - V_{\mathrm{TL}}}{I + (R_{n0} + \varepsilon_n \cdot t)}, \quad T_{\mathrm{Df}} = C_{\mathrm{plate}} \frac{V_{\mathrm{TL}} - V_{\mathrm{TH}}}{-I + (R_{n0} + \varepsilon_n \cdot t)} \tag{40}$$

  and oscillation period T_D of the measurement interface becomes

$$T_{\mathrm{D}} = T_{\mathrm{Dr}} + T_{\mathrm{Df}} = \frac{2C_{\mathrm{plate}} \left(V_{\mathrm{TH}} - V_{\mathrm{TL}}\right) I}{I^2 - (R_{n0} + \varepsilon_n \cdot t)^2} \tag{41}$$

  From (28) and (41) we can calculate the relative measurement error (period):

$$T_r = \frac{T_{\mathrm{D}} - T_{\mathrm{N}}}{T_{\mathrm{N}}} = \frac{I^2}{I^2 - (R_{n0} + \varepsilon_n \cdot t)^2} - 1 = \frac{((R_{n0} + \varepsilon_n \cdot t))^2}{I^2 - (R_{n0} + \varepsilon_n \cdot t)^2} \tag{42}$$

  with the parameters T_D and T_N that refer to the Figure 8.

S-FE

- Also in this last front-end analyzed a current of noise that varies linearly changes rising S_r and falling S_f slopes

$$S_r = \frac{I + (R_{n0} + \varepsilon_n \cdot t)}{C_{\mathrm{plate}}}, \quad S_f = \frac{-I + (R_{n0} + \varepsilon_n \cdot t)}{C_{\mathrm{plate}}} \tag{43}$$

  but we notice yet that slope magnitude average S_a is invariant to $\varepsilon_I \cdot t$

$$S_a = \frac{|S_r| + |S_f|}{2} = \frac{1}{2} \left(\frac{I + (R_{n0} + \varepsilon_n \cdot t)}{C_{\mathrm{plate}}} - \frac{-I + (R_{n0} + \varepsilon_n \cdot t)}{C_{\mathrm{plate}}} \right) = \frac{I}{C_{\mathrm{plate}}} \tag{44}$$

  Hence, using (44) we can calculate C_{plate} rejecting linearly varying noise current as common mode signals by measuring the slope of two adjacent charge-discharge ramps.

7 Experimental results

Introduction to results

The results proposed below are divided into two subsections. In Subsection 7.1 is shown the calculation of **sensitivity** as a variation of the output signal (as period of oscillation or slope of the ramp, depending on the front-end) for small variations of the plate capacitance (0.1%).

In Subsection 7.2 is shown the calculation of **sensitivity** as a variation of the same output signal in relation to the variations of the noise component: similarly, the measured capacitance variations have been calculated in relation to the same variations of the noise component.

In Figure 14 (with regard to circuits 6, 9 and 11) are provided and collected all the settings of the simulations made on LTspice [3], for each front-end, with regard to sensitivity as a variation of the output signal for small variations of the plate capacitance: the numerical values in the directives for the analysis of the transient response are guidelines.

RC-FE

```
.OPTIONS maxord=1
.OPTIONS itl1=1000
.OPTIONS itl2=1000
.OPTIONS itl4=1000
.OPTIONS numdgt=99
.OPTIONS measdgt=99
.OPTIONS vntol=1e-12
.OPTIONS reltol=1e-10
.OPTIONS gmin=1e-15
.OPTIONS abstol=1e-15
.OPTIONS plotwinsize=0

.ic V(Vc)=3.34V

.tran 0 0.04s 0 1us
.save V(Vout)
```

IC-FE

```
.OPTIONS maxord=1
.OPTIONS itl1=1000
.OPTIONS itl2=1000
.OPTIONS itl4=1000
.OPTIONS numdgt=99
.OPTIONS measdgt=99
.OPTIONS vntol=1e-12
.OPTIONS reltol=1e-10
.OPTIONS gmin=1e-15
.OPTIONS abstol=1e-15
.OPTIONS plotwinsize=0

.lib opamp.sub

.ic V(Vc)=1.65V

 Ic = if (V(v) > 2.5, -27nA, +27nA)

.tran 0 0.04s 0 1us
.save V(v)
```

S-FE

```
.OPTIONS maxord=1
.OPTIONS itl1=1000
.OPTIONS itl2=1000
.OPTIONS itl4=1000
.OPTIONS numdgt=99
.OPTIONS measdgt=99
.OPTIONS vntol=1e-12
.OPTIONS reltol=1e-10
.OPTIONS gmin=1e-15
.OPTIONS abstol=1e-15
.OPTIONS plotwinsize=0

.ic V(Vc)=-71.85V

Ic = if (V(Vdrive) > 2.5, -112.5nA, +112.5nA)

Vdrive = PULSE(0V 5V 0us 0.1us 0.1us 312.5us 625us 2000000000)

.tran 0 0.05s 0s 1us
.save V(Vc)
```

Figure 14: Simulation settings for each circuit for front-end sensitivities to capacitance variations

In Figure 15 (still with regard to circuits 6, 9 and 11) are provided and collected all the settings of the simulations made on LTspice [3], for each front-end, with regard to sensitivity as a variation of the same output signal or of the measured capacitance in relation to the variations of the noise component : the numerical values in the directives for the analysis of the transient response and for the sinusoid noise are guidelines.

RC-FE

```
.OPTIONS maxord=1
.OPTIONS itl1=1000
.OPTIONS itl2=1000
.OPTIONS itl4=1000
.OPTIONS numdgt=99
.OPTIONS measdgt=99
.OPTIONS vntol=1e-12
.OPTIONS reltol=1e-10
.OPTIONS gmin=1e-15
.OPTIONS abstol=1e-15
.OPTIONS plotwinsize=0

.ic V(Vc)=3.34V

Idrift = SINE(0 51n 1)

.tran 0 1s 0s 1us
.save V(Vout)
```

IC-FE

```
.OPTIONS maxord=1
.OPTIONS itl1=1000
.OPTIONS itl2=1000
.OPTIONS itl4=1000
.OPTIONS numdgt=99
.OPTIONS measdgt=99
.OPTIONS vntol=1e-12
.OPTIONS reltol=1e-10
.OPTIONS gmin=1e-15
.OPTIONS abstol=1e-15
.OPTIONS plotwinsize=0

.lib opamp.sub

.ic V(Vc)=1.79V

Ic = if (V(v) > 2.5, -27nA, +27nA)

Idrift = SINE(0 0.0027n 1)

.tran 0 0.6s 0s 1us
.save V(v)
```

S-FE

```
.OPTIONS maxord=1
.OPTIONS itl1=1000
.OPTIONS itl2=1000
.OPTIONS itl4=1000
.OPTIONS numdgt=99
.OPTIONS measdgt=99
.OPTIONS vntol=1e-12
.OPTIONS reltol=1e-10
.OPTIONS gmin=1e-15
.OPTIONS abstol=1e-15
.OPTIONS plotwinsize=0

.ic V(Vc)=-71.85V

Vdrive = PULSE(0V 5V 0us 0.1us 0.1us 312.5us 625us 2000000000)

Ic = if (V(Vdrive) > 2.5, -112.5nA, +112.5nA)

Idrift = SINE(0 1.125n 1)

.tran 0 1s 0s 1us
.save V(Vc)
```

Figure 15: Simulation settings for each circuit for front-end sensitivity to noise frequency

7.1 Front-end sensitivities to capacitance variations

As already introduced, for each front-end for small variations of the plate capacitance (0.1%) the corresponding variation of the output signal (such as the oscillation period or the slope of the ramp, depending on the front-end) was measured.

In the following, the letters indicating the period and the capacitance (T,C) with the subscript "reference" will refer to the measurements and calculations made with the nominal value of the capacitance of the plate while those without will refer to the measurements and calculations made with the capacitance of the plate varied by 0.1%.

Table 8 shows the capacitance values of the plate in both cases:

	RC-FE	IC-FE	S-FE
$C_{reference}$ [pF]	60	6	25
C' [pF]	60.06	6.006	25.025

Table 8: Plate capacitance values used in the simulations

Table 9 shows the values of the output frequency obtained both in the nominal case and with the capacitance of the plate varied by 0.1%:

	RC-FE	IC-FE
$f_{reference}$ [kHz]	18.07919	1.60761
f' [kHz]	18.06117	1.60600

Table 9: Output signals obtained both in the nominal case and with the capacitance of the plate varied by 0.1%

and Table 10 shows the slope output for the slope modulator front-end.

	S-FE
$S_{reference}$ [kV/s]	4.49999
S' [kV/s]	4.49550

Table 10: Output signals obtained both in the nominal case and not

Then I calculate the sensitivity value as a variation of the output signal for a small change in plate capacitance.

With regard to front-end RC-FE and IC-FE, the value of the sensitivity was calculated with the following mathematical expression:

$$S = \left| \frac{\frac{f' - f_{\text{reference}}}{f_{\text{reference}}}}{\frac{C' - C_{\text{reference}}}{C_{\text{reference}}}} \right| \tag{45}$$

As far as the S-FE front-end is concerned, the value of the sensitivity has been calculated in the same way, bearing in mind that the output signal is a ramp slope and not an oscillation period as in the case of front-end RC-FE and IC-FE:

$$S = \left| \frac{\frac{S' - S_{\text{reference}}}{S_{\text{reference}}}}{\frac{C' - C_{\text{reference}}}{C_{\text{reference}}}} \right| \tag{46}$$

It should be noted that the differences calculated are not absolute differences but relative differences to be able to compare the sensitivities of the various front-ends.

In Table 11 the calculated sensitivity values:

	RC-FE	IC-FE	S-FE
Output sensitivity	0.99636	0.99707	0.99900

Table 11: Front-end output sensitivities to capacitance variations

The Figure 16 shows the sensitivity in comparison for the 3 types of front-end as a variation of the output signal for small variations of the plate capacitance.

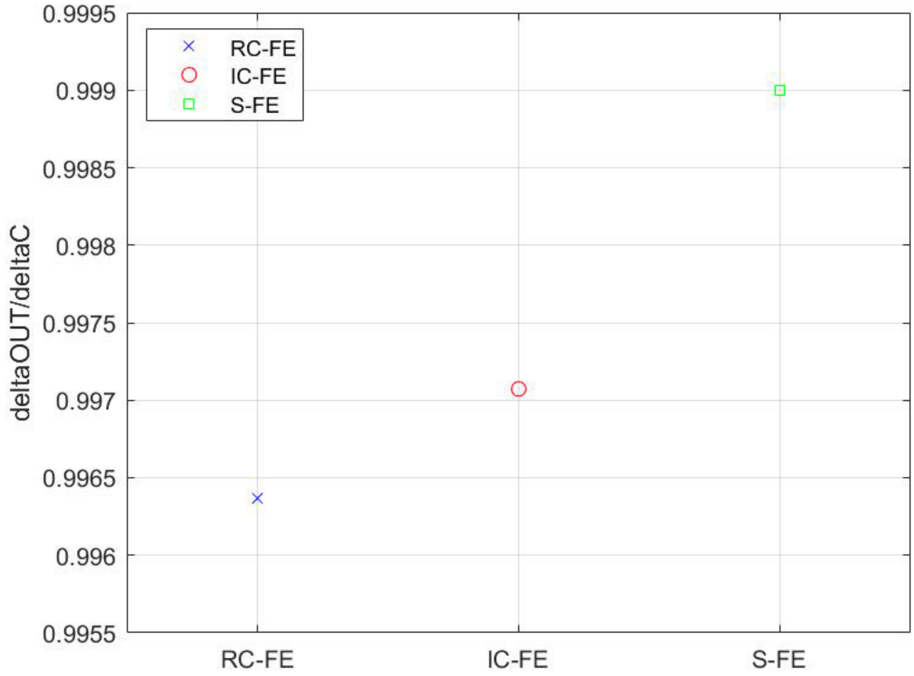

Figure 16: Simulation values of sensitivity to capacity variation for the different front-ends

7.2 Front-end sensitivity to noise frequency

Noise has been inserted at each front-end using a **current source** (sinusoid of a certain amplitude and frequency) in parallel to the capacitance to see what effect they have on capacitance measurement and front-end output for each of the circuits. The effect of noise is a **variation** of the oscillation period for the RC-FE and IC-FE, or the slope of the S-FE ramp.

Table 12 shows the nominal capacitance values of the plate included in the simulations for the front-end sensitivity to noise frequency for the different front-ends:

	RC-FE	IC-FE	S-FE
C_{nominal} [pF]	60	25	25

Table 12: Nominal plate capacitance values used in the simulations

Please note that the noise frequencies of interest are very low, from a few Hz down, because we are interested mostly to eliminate drift (from tenths to thousandths of Hz or DC). The frequency values of the noise sinusoid are as follows: 5 Hz, 1 Hz, 0.5 Hz e 0.1 Hz. For each frequency of the noise input signal has been calculated:

- the sensitivity of the capacitance calculation as $\dfrac{\Delta C_{\text{p}}}{\Delta I_{\text{p}}}$
- the relative sensitivity of the front-end output such as $\dfrac{\Delta T_{\text{p}}/T_{\text{p,ref}}}{\Delta I_{\text{p}}/I_{\text{p,ref}}}$ or $\dfrac{\Delta S_{\text{p}}/S_{\text{p,ref}}}{\Delta I_{\text{p}}/I_{\text{p,ref}}}$ depending on front-end

where ΔI_{p} is the change in the amplitude of the disturbing signal (the current sinusoid), ΔC_{p} is the measured capacitance variation due to the input noise signal and ΔT_{p} or ΔS_{p} is the variation of the front-end output (period or slope) for the same noise.

7.2.1 Sensitivity of front-end output & capacitance calculation

RC period modulator (RC-FE)

For each frequency value (5 Hz, 1 Hz, 0.5 Hz e 0.1 Hz), a first nominal sine wave amplitude of 50 nA was applied and then, for the same frequency values, a slightly varied sine wave amplitude of 51nA was applied.

I' [nA]	$I_{reference}$ [nA]
51	50

Table 13: Amplitude values of the noise signal for the reference case and not (RC-FE)

The first check carried out was to verify whether the front-end output (period) and similarly the calculated plate capacitance had a sinusoidal trend. Please note that the effect of sinusoidal noise is a variation of the output oscillation period in this case and of the capacitance calculated in a similar way as you can see in Figures 17 and 18. From the amplitude definition, the references for the measurement of amplitudes, due to the disturbance, are shown on Figure 17 for the output period and on Figure 18 for the plate capacity.

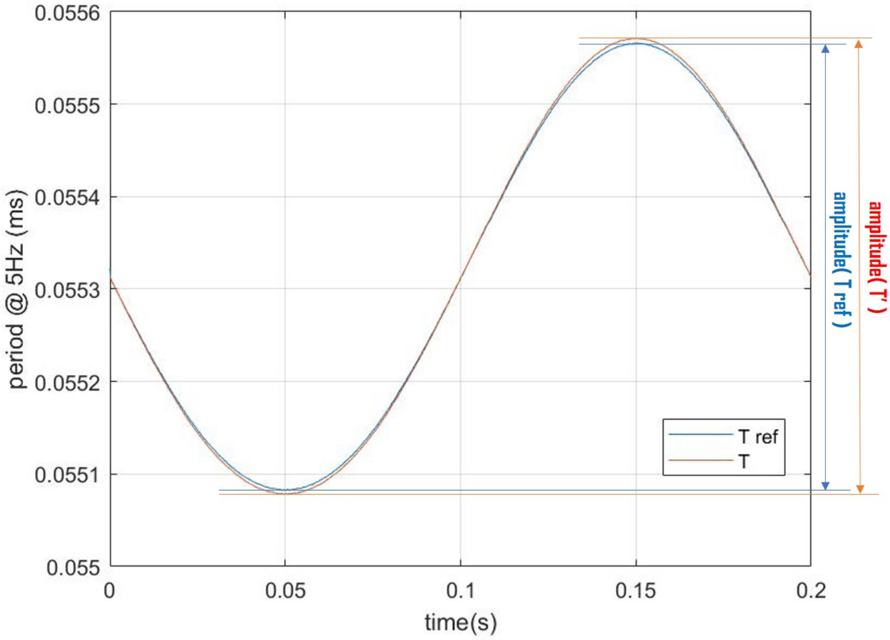

Figure 17: Variation of the output oscillation period at 5 Hz noise (RC-FE)

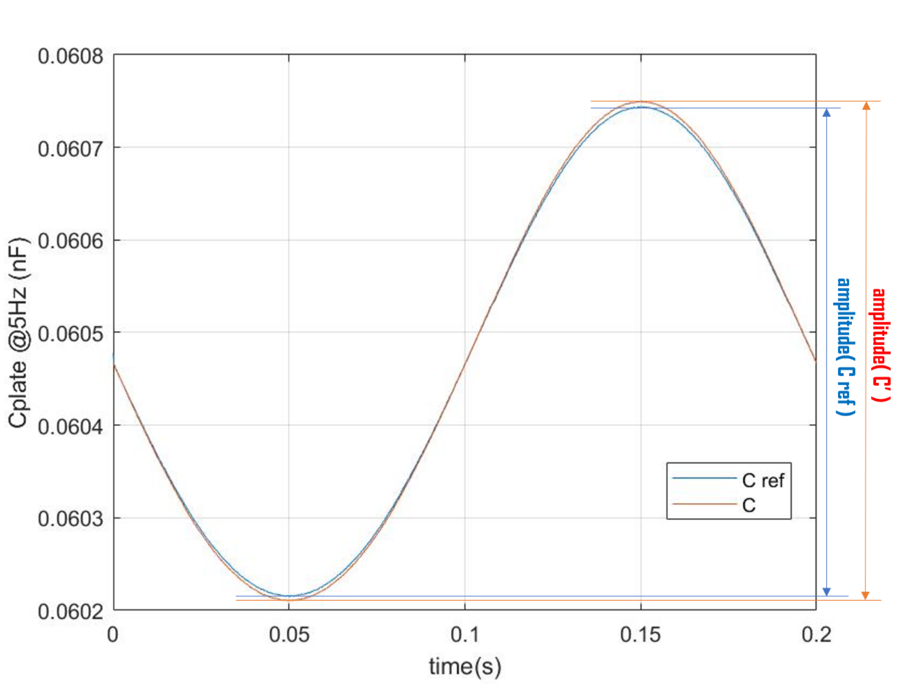

Figure 18: Variation of the calculated capacitance at 5 Hz noise (RC-FE)

Therefore, to measure the noise effect, the simulation data were processed and the two sensitivity values (for each frequency) were calculated according to the following expressions:

- the relative sensitivity of the front-end output such as $\dfrac{\Delta T_{\mathrm{p}}/T_{\mathrm{p,ref}}}{\Delta I_{\mathrm{p}}/I_{\mathrm{p,ref}}}$

  In particular:

$$S_{\mathrm{T,rel}} = \frac{\frac{amplitude(T')-amplitude(T_{\mathrm{reference}})}{amplitude(T_{\mathrm{reference}})}}{\frac{amplitude(I')-amplitude(I_{\mathrm{reference}})}{amplitude(I_{\mathrm{reference}})}} \tag{47}$$

- the sensitivity of the capacitance calculation as $\dfrac{\Delta C_{\mathrm{p}}}{\Delta I_{\mathrm{p}}}$

  In particular:

$$S_{\mathrm{C}} = \frac{amplitude(C') - amplitude(C_{\mathrm{reference}})}{amplitude(I') - amplitude(I_{\mathrm{reference}})} \tag{48}$$

where ΔI_{p} is the change in the amplitude of the disturbing signal (the current sinusoid), ΔC_{p} is the measured capacitance variation due to the input noise signal and ΔT_{p} is the variation of the front-end output (period) for the same noise.

The "reference" subscript refers to the quantities in the case of the nominal sinusoid amplitude value.

In Tables 14 and 15 the amplitude data measured as you can see from the Figures 17 and 18.

Front-end period output:

noise freq. [Hz]	T' [us]	$T_{\mathrm{reference}}$ [us]	ΔT_{p} [us]
5	0.49353614	0.48406637	0.0094697759
1	0.49397721	0.48410399	0.0098732262
0.5	0.49397996	0.48422952	0.0097504347
0.1	0.49416306	0.48439225	0.0097708047

Table 14: Period for the two amplitude values and for each frequency of the noise signal and their respective absolute difference (RC-FE)

Calculated capacitance:

noise freq. [Hz]	C' [pF]	$C_{reference}$ [pF]	ΔC_p [pF]
5	0.53952	0.52917	0.010352
1	0.54000	0.52921	0.010793
0.5	0.54001	0.52935	0.010659
0.1	0.54021	0.52952	0.010681

Table 15: Capacitance for the two amplitude values and for each frequency of the noise signal and their respective absolute difference (RC-FE)

In Tables 16 and 17 the calculated sensitivity values.

noise freq. [Hz]	$S_{T,rel}$
5	0.9781450
1	1.0197422
0.5	1.0067988
0.1	1.0085632

Table 16: Relative sensitivity, for each frequency, of the front-end output (RC-FE-based)

noise freq. [Hz]	S_C [pF/nA]
5	0.0103521
1	0.0107932
0.5	0.0106590
0.1	0.0106812

Table 17: Sensitivity values, for each frequency, of capacitance calculation (RC-FE-based)

Figure 19 shows the trend of delta T as a function of noise frequency.

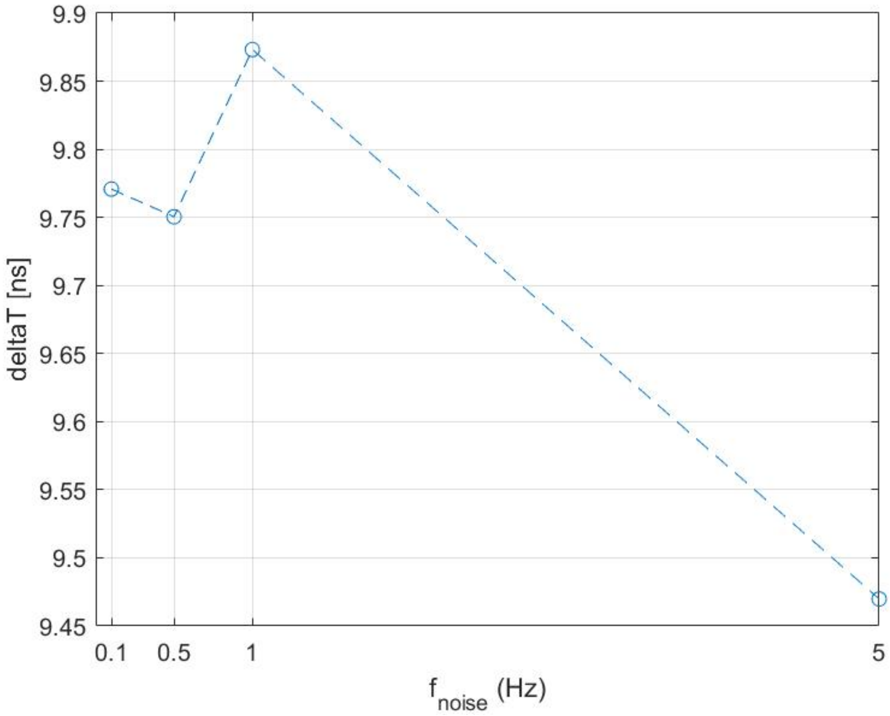

Figure 19: Changes of oscillation period function of f_{noise} for RC-FE

In Fig. 20 and 21 are plotted the values of the Tables 16 and 17 in order to give a qualitative trend of the sensitivity value as the frequency increases (as the period decreases).

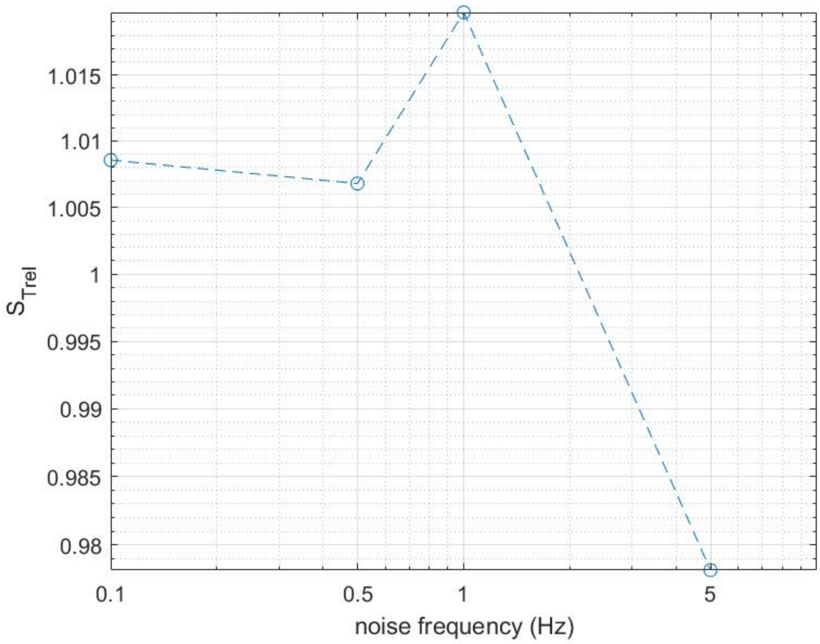

Figure 20: Sensitivity of the front-end output as the noise frequency decreases for RC-FE

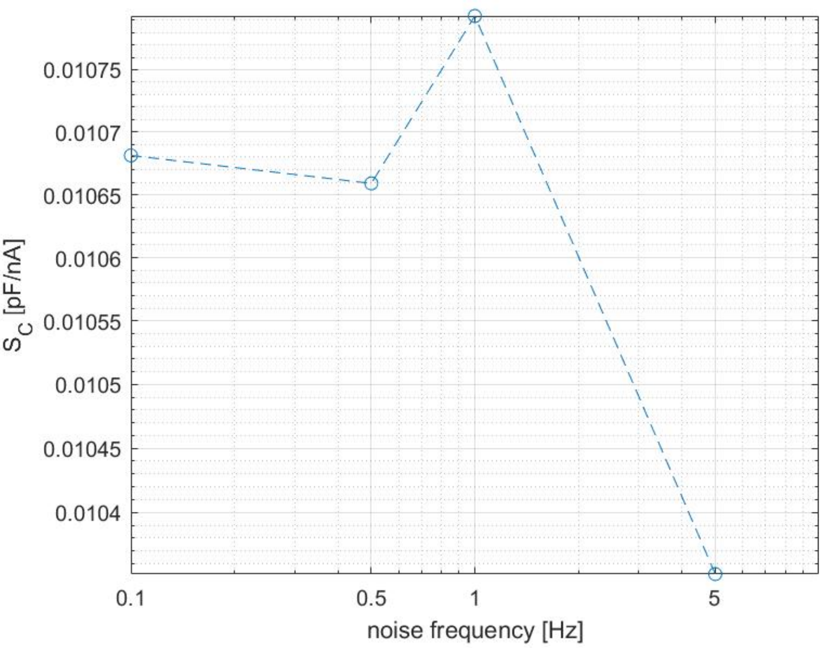

Figure 21: Sensitivity of the capacitance calculation to decreasing noise frequency for RC-FE

Constant current period modulator (IC-FE)

Similarly to what was done for the front-end based on the RC-FE, on the front-end based on the IC-FE, for each frequency value specified before, two noise sinusoids were applied to the circuit: first the one with the nominal amplitude value (0.0027 nA) and then the one with an amplitude value changed to 0.0030 nA.

I' [nA]	$I_{reference}$ [nA]
0.0030	0.0027

Table 18: Amplitude values of the noise signal (IC-FE)

For each of them the circuit has been simulated and to measure the effect of the noise, data from the simulations have been processed. Also in this case the effect of sinusoidal noise is a variation of the output oscillating period of the front-end also in this case.

Before carrying out the same calculations, the sensitivity values, which are equal to those of the front-end based on the RC-FE (taking into account the different values of the output period, the calculated capacitance and the input noise sine wave amplitude), were verified that the values of interest of the circuit had a sinusoidal trend.

In fact, it is remarked again, that the effect of sinusoidal noise is a variation of the output oscillation period in this case and of the capacitance calculated in a similar way as you can see in Figures 22 and 23. From the amplitude definition, the references for the measurement of amplitudes, due to the disturbance, are shown on Figure 22 for the output period and on Figure 23 for the plate capacity.

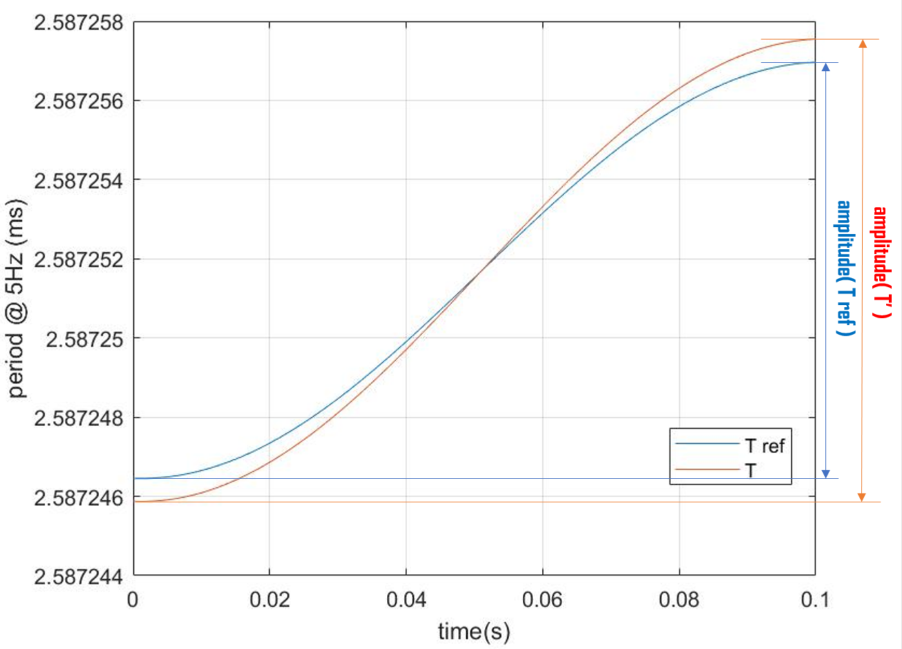

Figure 22: Variation of the output oscillation period at 5 Hz noise (IC-FE)

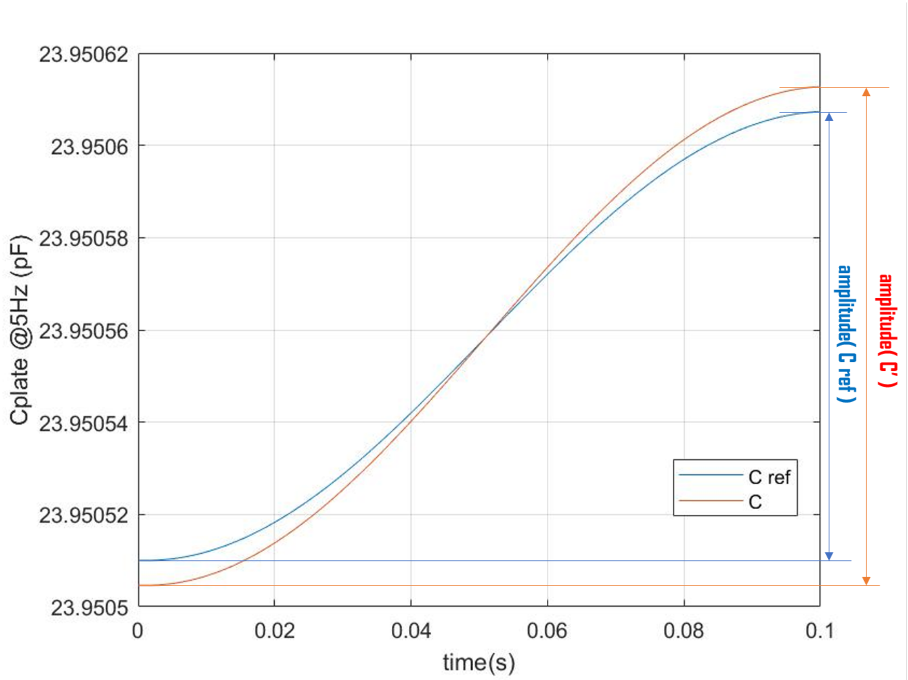

Figure 23: Variation of the calculated capacitance at 5 Hz noise (IC-FE)

Once again it should be noted that "reference" refers to the measured/calculated quantities in the case of nominal sinusoid amplitude namely 0.0027 nA.

In Tables 19 and 20 the amplitude data measured as you can see from the Figures 22 and 23.

Front-end period output:

noise freq. [Hz]	T' [ns]	$T_{reference}$ [ns]	ΔT_p [ns]
5	11.67769	10.51053	1.167164
1	2.33611	2.10337	0.232739
0.5	1.16834	1.05450	0.113834
0.1	0.23855	0.21369	0.024860

Table 19: Period for the two amplitude values and for each frequency of the noise signal and their respective absolute difference (IC-FE)

Calculated capacitance:

noise freq. [Hz]	C' [fF]	$C_{reference}$ [fF]	ΔC_p [fF]
5	0.1081021	0.0972975	0.01080460
1	0.0216257	0.0194712	0.00215450
0.5	0.0108155	0.0097617	0.00105377
0.1	0.0022083	0.0019781	0.00023013

Table 20: Capacitance for the two amplitude values and for each frequency of the noise signal and their respective absolute difference (IC-FE)

Below are the sensitivity values of the capacitance calculation and the front-end output (as done for the circuit based on the RC-FE).

The expressions used for the sensitivity calculation (which are the same as those used for the RC-FE-based sensitivity calculation (47) and (48)):

- the relative sensitivity of the front-end output such as $\dfrac{\Delta T_p / T_{p,ref}}{\Delta I_p / I_{p,ref}}$

  In particular:

$$S_{\mathrm{Trel}} = \frac{\frac{amplitude(T') - amplitude(T_{\mathrm{reference}})}{amplitude(T_{\mathrm{reference}})}}{\frac{amplitude(I') - amplitude(I_{\mathrm{reference}})}{amplitude(I_{\mathrm{reference}})}} \tag{49}$$

- the sensitivity of the capacitance calculation as $\dfrac{\Delta C_{\mathrm{p}}}{\Delta I_{\mathrm{p}}}$

  In particular:

$$S_{\mathrm{C}} = \frac{amplitude(C') - amplitude(C_{\mathrm{reference}})}{amplitude(I') - amplitude(I_{\mathrm{reference}})} \tag{50}$$

where ΔI_{p} is the change in the amplitude of the disturbing signal (the current sinusoid), ΔC_{p} is the measured capacitance variation due to the input noise signal and ΔT_{p} is the variation of the front-end output (period) for the same noise.

In Tables 21 and 22 the calculated sensitivity values.

noise freq. [Hz]	$\mathrm{S}_{\mathrm{T,rel}}$
5	0.999423
1	0.995856
0.5	0.971549
0.1	1.047045

Table 21: Relative sensitivity, for each frequency, of the front-end output (IC-FE-based)

noise freq. [Hz]	S_{C} [pF/nA]
5	0.03601534
1	0.00718167
0.5	0.00351259
0.1	0.00076713

Table 22: Sensitivity values, for each frequency, of capacitance calculation (IC-FE-based)

Figure 24 shows the trend of delta T as a function of noise frequency.

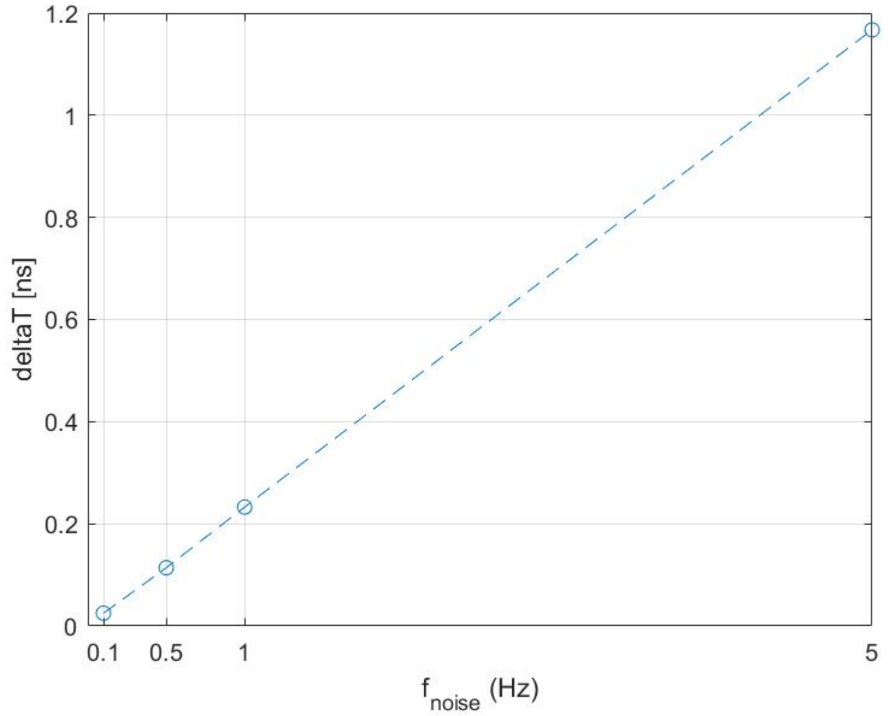

Figure 24: Changes of oscillation period function of f_{noise} for IC-FE

The Figures 25 and 26 showing the increasing frequency trend of the values of sensitivity of the capacitance calculation and the front-end output.

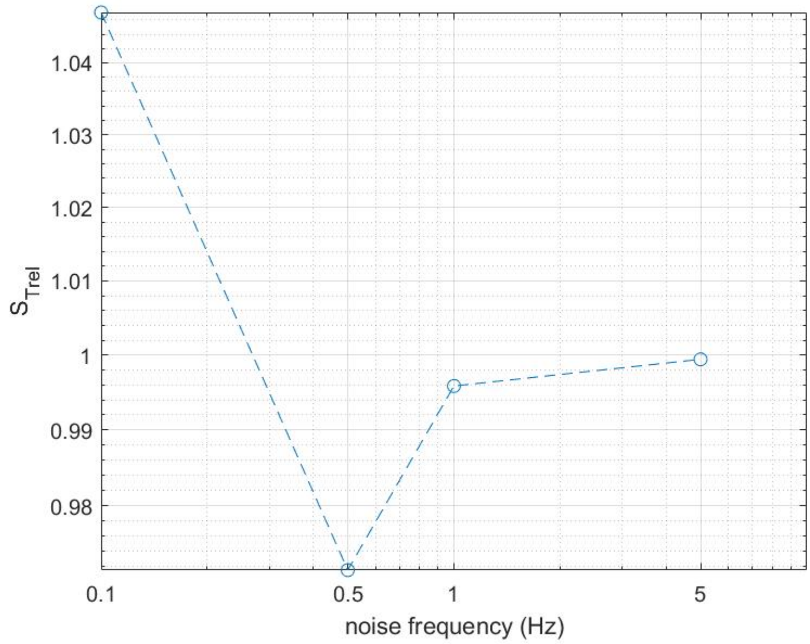

Figure 25: Sensitivity of the front-end output as the noise frequency decreases for IC-FE

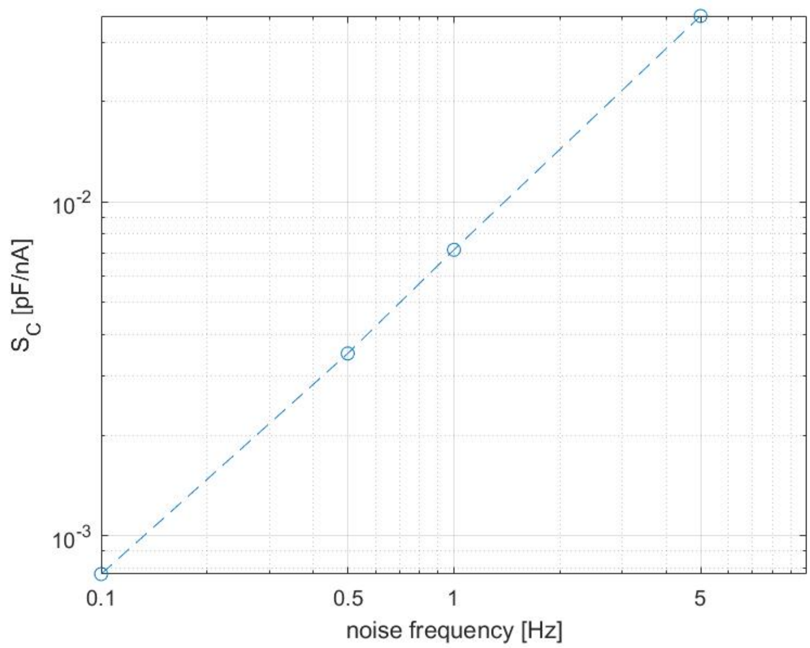

Figure 26: Sensitivity of the capacitance calculation to decreasing noise frequency for IC-FE

Constant current slope modulation (S-FE)

For this front-end the above speeches and considerations, as well as the calculations for the sensitivity of the capacitance and the output of the front-end, remain unchanged: the only difference is that the output signal of the front-end is not an oscillation period but the slope of the ramp. Here the nominal value of the sine wave amplitude of noise is 1.125 nA while the changed value is of 1.135 nA.

I' [nA]	$I_{reference}$ [nA]
1.135	1.125

Table 23: Amplitude values of the noise signal for the reference case and not (S-FE)

Please note that also here the effect of sinusoidal noise is a variation of the output oscillation that in this case is the slope of the ramp and as always of the capacitance calculated in a similar way as you can see in Figures 27 and 28. From the amplitude definition, the references for the measurement of amplitudes, due to the disturbance, are shown on Figure 27 for the output slope and on Figure 28 for the plate capacity.

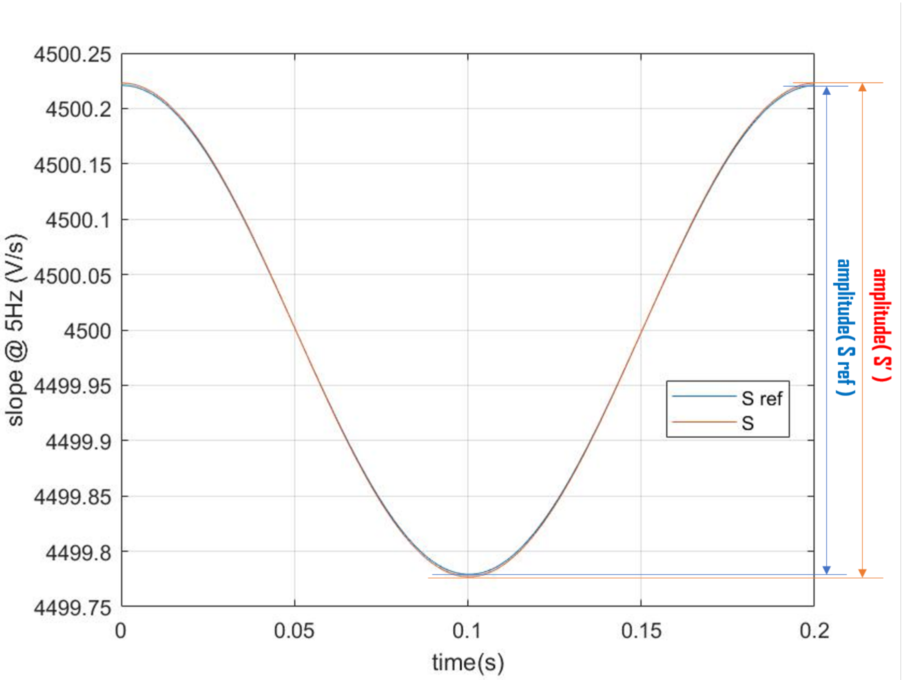

Figure 27: Variation of the output oscillation slope at 5 Hz noise (S-FE)

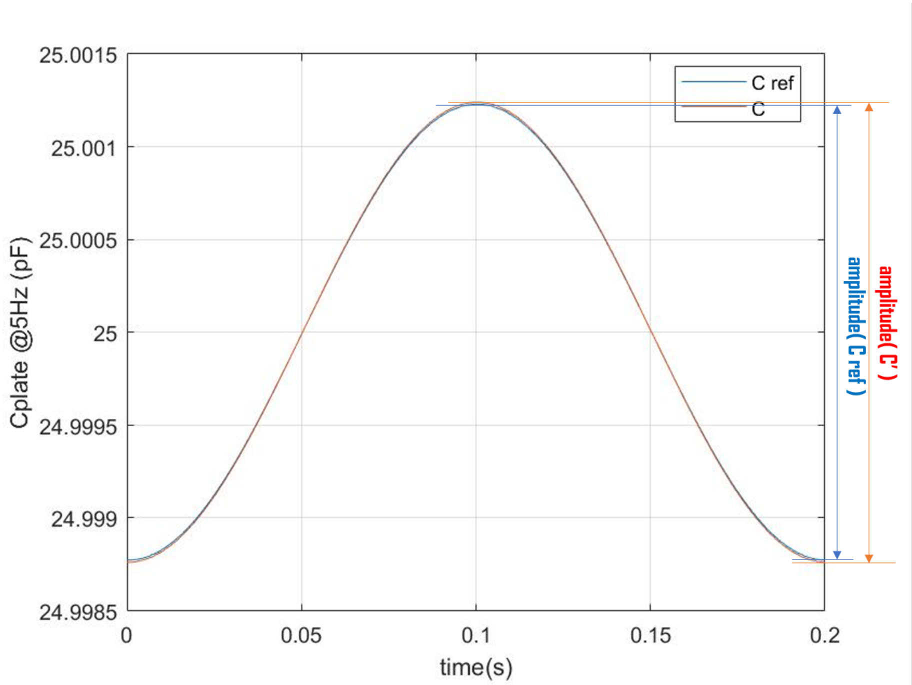

Figure 28: Variation of the calculated capacitance at 5 Hz noise (S-FE)

Therefore, the sensitivity value of the front-end output should be calculated as follows because the output characteristic is the slope:

- the relative sensitivity of the front-end output such as $\dfrac{\Delta S_{\mathrm{p}}/S_{\mathrm{p,ref}}}{\Delta I_{\mathrm{p}}/I_{\mathrm{p,ref}}}$

  In particular:

$$S_{\mathrm{S,rel}} = \frac{\frac{amplitude(S')-amplitude(S_{\mathrm{reference}})}{amplitude(S_{\mathrm{reference}})}}{\frac{amplitude(I')-amplitude(I_{\mathrm{reference}})}{amplitude(I_{\mathrm{reference}})}} \tag{51}$$

While the sensitivity value of the capacitance calculation has been calculated with the same formula (48):

- the sensitivity of the capacitance calculation as $\dfrac{\Delta C_{\mathrm{p}}}{\Delta I_{\mathrm{p}}}$

  In particular:

$$S_{\mathrm{C}} = \frac{amplitude(C') - amplitude(C_{\mathrm{reference}})}{amplitude(I') - amplitude(I_{\mathrm{reference}})} \tag{52}$$

where ΔI_{p} is always the change in the amplitude of the disturbing signal (the sinusoid), ΔC_{p} is always the measured capacitance excursion due to the input noise signal but ΔS_{p} is the variation of the front-end output (in this case the slope) for the same reason.

In Tables 24 and 25 the amplitude data measured.

Front-end slope output:

noise freq. [Hz]	S' [V/s]	$S_{\mathrm{reference}}$ [V/s]	ΔS_{p} [V/s]
5	0.4457093	0.4417823	0.003926955
1	0.0891427	0.0883573	0.000785398
0.5	0.0445718	0.0441791	0.000392700
0.1	0.0089182	0.0088397	0.000078539

Table 24: Slope for the two amplitude values and for each frequency of the noise signal and their respective absolute difference (S-FE)

Calculated capacitance:

noise freq. [Hz]	C' [fF]	$\mathrm{C_{reference}}$ [fF]	ΔC_{p} [fF]
5	2.476163	2.454346	0.02181642
1	0.495237	0.490873	0.00436332
0.5	0.247621	0.245439	0.00218166
0.1	0.049545	0.049109	0.00043633

Table 25: Capacitance for the two amplitude values and for each frequency of the noise signal and their respective absolute difference (S-FE)

As for all front-ends, we can find the values of the different sensitivity components in Table 26 and 27 and their Figures 30 and 31 to compare them qualitatively and see the trend as the frequency of the noise component increases.

noise freq. [Hz]	$\mathrm{S_{S,rel}}$
5	1.00000029831
1	1.00000000192
0.5	0.99999201329
0.1	0.99954892841

Table 26: Relative sensitivity, for each frequency, of the front-end output (S-FE-based)

noise freq. [Hz]	$\mathrm{S_C}$ [pF/nA]
5	0.002181642
1	0.000436332
0.5	0.000218166
0.1	0.000043633

Table 27: Sensitivity values, for each frequency, of capacitance calculation (S-FE-based)

Figure 29 shows the trend of delta S as a function of noise frequency.

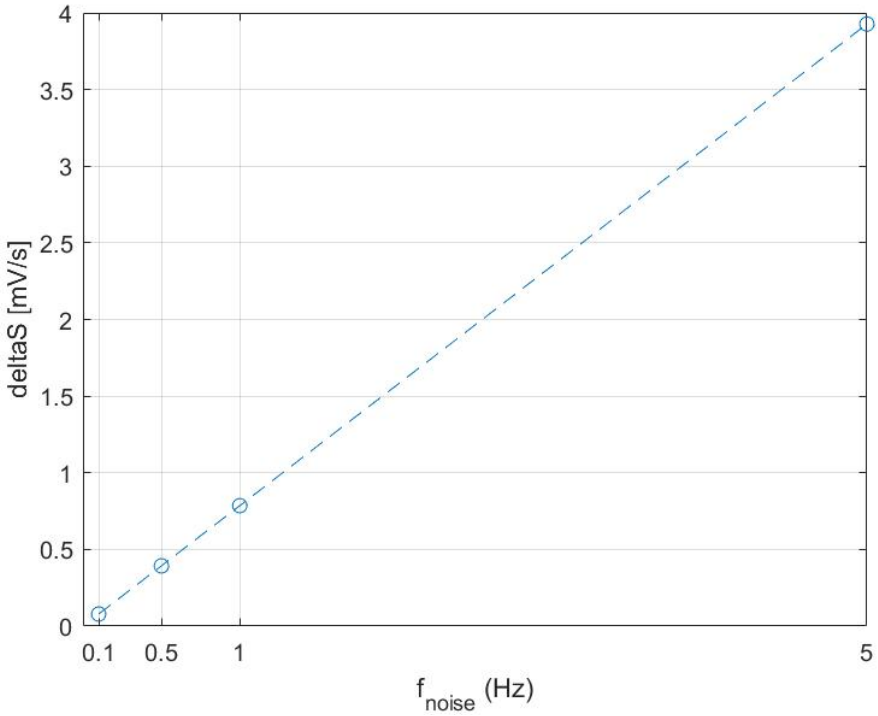

Figure 29: Changes of ramp slope function of f_{noise} for S-FE

The Figures 30 and 31 showing the increasing frequency trend of the values of sensitivity of the capacitance calculation and the front-end output.

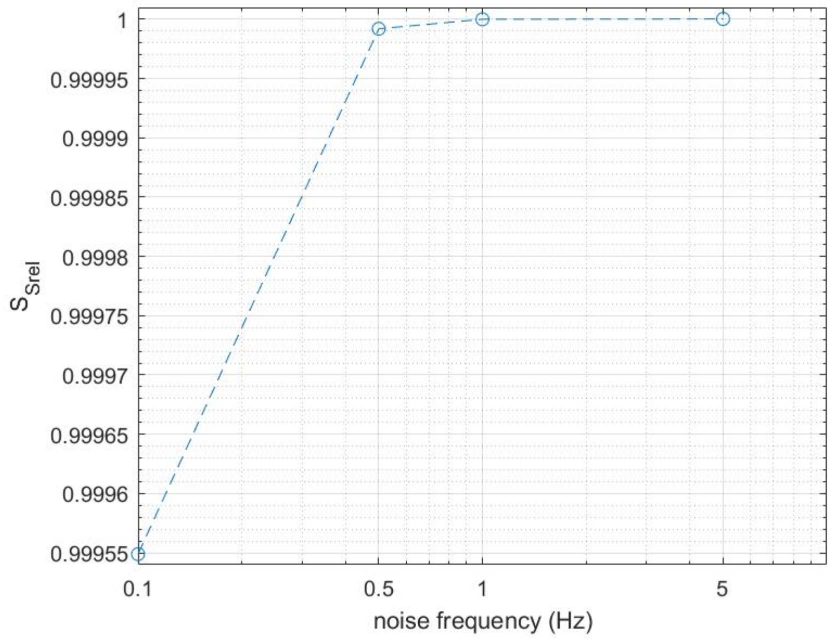

Figure 30: Sensitivity of the front-end output as the noise frequency decreases for S-FE

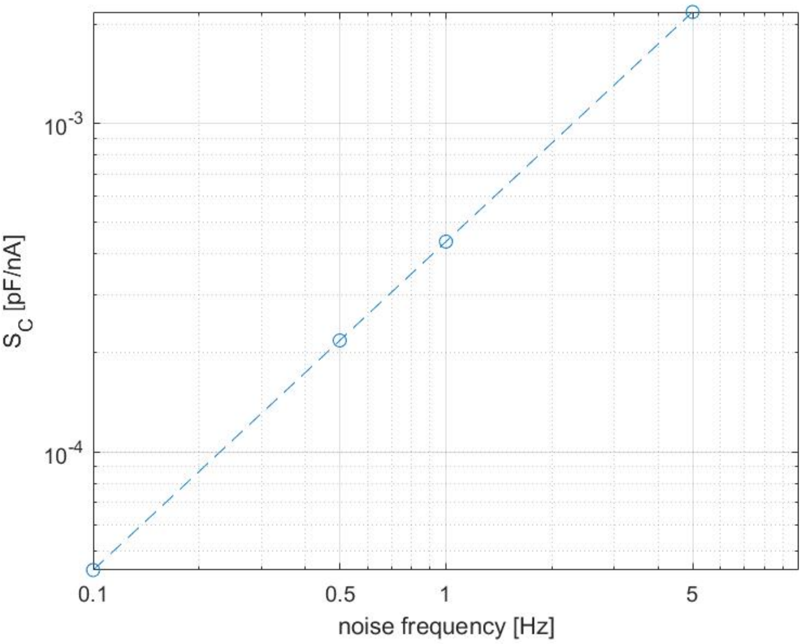

Figure 31: Sensitivity of the capacitance calculation to decreasing noise frequency for S-FE

8 Result discussion

Below the different sensitivities calculated so far (analytically and with Spice simulations) have been compared with the help of Figures to see their value in comparison as in the case without noise or their trend in decreasing frequency as in the case with input noise.

8.1 Sensitivity to capacitance variation: comparison between analytical calculations and simulations

Below the sensitivity in comparison for the 3 types of front-end, both analytically and through simulations, as a variation of the output signal for small variations of the plate capacitance.

The measured/calculated data and the formulas used can be found in the reference Sections 6.1 and 7.1.

In Table 28 comparable results were obtained with the analytical calculation by comparing them with those of the simulations (in brackets).

	RC-FE	IC-FE	S-FE
Output sensitivity	1.00777 (0.99636)	0.95967 (0.99707)	1.00000 (0.99900)

Table 28: Absolute value of front-end output sensitivities to capacitance variations calculated compared with relative difference

In Fig.32 the analytical results were compared with the simulations also graphically for the 3 types of front-end.

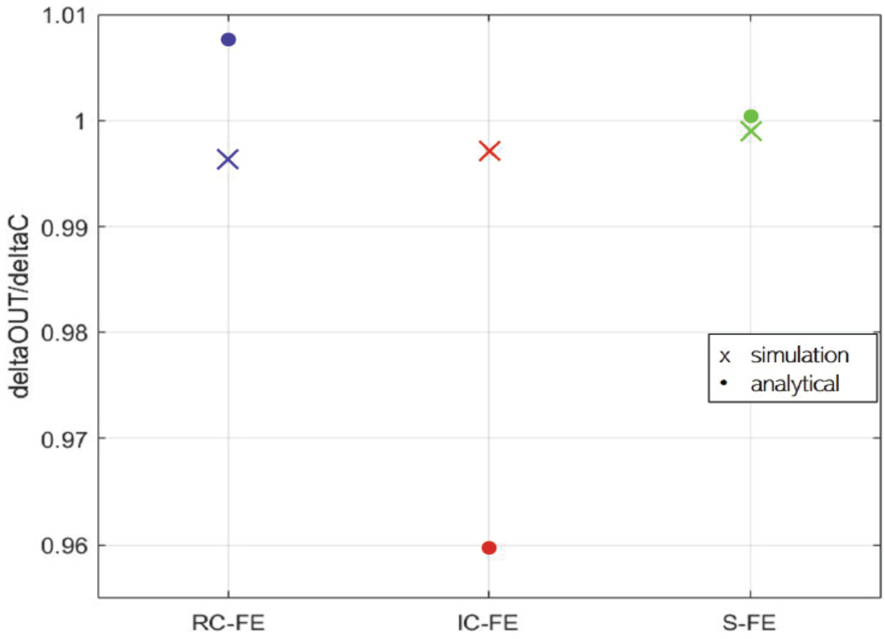

Figure 32: Comparison between analytical and simulations results of front-end output sensitivities to input capacitance variations

The results obtained through the simulations are close to those obtained through the analytical calculations, deviating only by 3-5 %. The sensitivity is around 1 for all three front-ends: the S-FE analytical one is lower than the RC-FE one while the lowest of all is that of IC-FE.

8.2 Sensitivity of capacitance calculation & front-end output with noise

Now, we are able to compare the sensitivities of the various front-ends. The measured/calculated data of the amplitudes are shown in subsubsection 7.2.1.

The relative sensitivity of the front-ends output as $\dfrac{\Delta T_{\mathrm{p}}/T_{\mathrm{p,ref}}}{\Delta I_{\mathrm{p}}/I_{\mathrm{p,ref}}}$ or $\dfrac{\Delta S_{\mathrm{p}}/S_{\mathrm{p,ref}}}{\Delta I_{\mathrm{p}}/I_{\mathrm{p,ref}}}$ (depending on front-end), calculated respectively in (47), (49) and (51).

The Figure 33 shows the sensitivity values of the output of the front-ends for the different frequencies compared (sensitivity intended as a variation of the output signal compared to the same variations of the noise component).

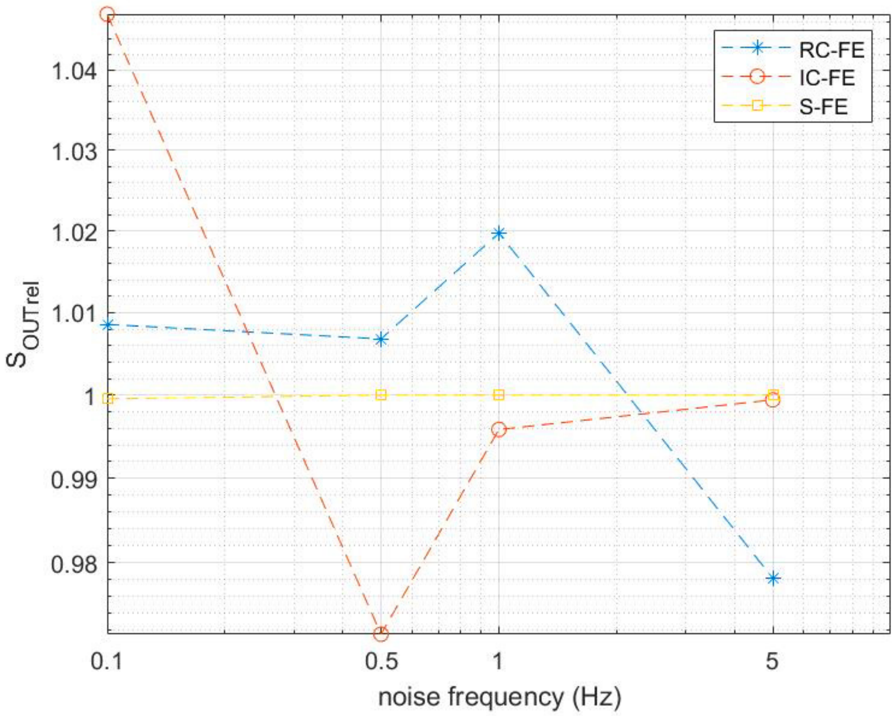

Figure 33: Values of sensitivity of front-ends output at different noise frequencies

Fig. 33 shows that the sensitivity to changes in noise amplitude does not change with frequency: meaning that the variation in sensitivity to noise amplitude variations is really very small with frequency because there is a slight oscillation in the results, as can be seen from the Figure 33, but this phenomenon is probably due to measurement errors.

The sensitivity of the capacitance calculation as $\dfrac{\Delta C_{\mathrm{p}}}{\Delta I_{\mathrm{p}}}$ is calculated in (48), (50) and (52).

The Fig. 34 shows the sensitivity of the capacitance calculation as measured capacitance changes in relation to changes in the noise component.

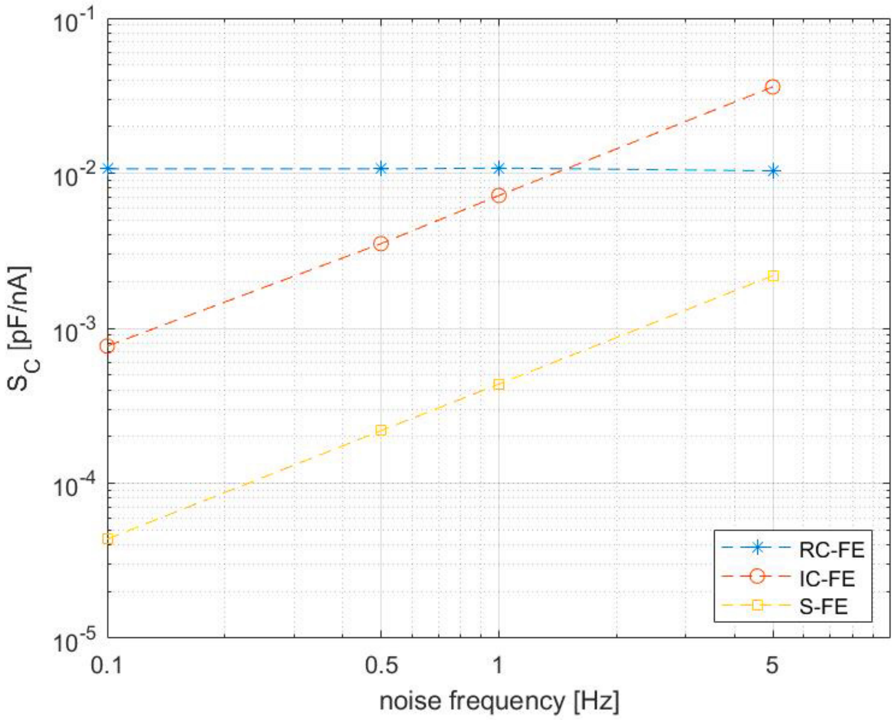

Figure 34: Values of sensitivity of capacitance calculation for the different front-ends at different noise frequencies

Fig. 34 shows that the error introduced by the noise on the measurement (of the capacity) is almost constant with the frequency for RC-FE, while it decreases proportionally with the lowering of the noise frequency for IC-FE and S-FE and is much lower for the last one.

9 Conclusions and future work

It has been concluded that the three front-ends have different characteristics in terms of sensitivity both as a variation of the output signal for small variations of the armature capacity and above all in terms of sensitivity as variations of the output signal or similarly of the measured capacity in relation to the variations of the noise component on which we have focused more.

In particular, S-FE shows a greater rejection to the noise component than RC-FE and IC-FE while losing in terms of sensitivity with respect to location.

Therefore these significant results regarding the study and characterisation of these three front-ends can be taken as the reference point for subsequent research work and in particular starting from these results in order to be able to choose one front-end rather than another by virtue of its sensitivity values studied and validated both with simulations and analytically in this treatment: for example, S-FE can be chosen because of its higher rejection to long environmental noise rather than IC-FE or RC-FE, perhaps losing in terms of sensitivity with respect to small variations in the output signal or in other words the precision with which it is possible to locate a subject.

This and many other considerations can be made at the beginning of the next research work and on the basis of my results it will be possible to discern the most suitable front-end to start another experimental work.

References

[1] P. Alloatti. Low power operation of indoor sensors for human localization. *Supervisors: Luciano Lavagno, Mihai Teodor Lazarescu*, 2019.

[2] A. Bellinaso. Machine learning algorithms for human localization using long distance capacitive and infrared sensors. *Supervisors: Luciano Lavagno, Mihai Teodor Lazarescu*, 2017.

[3] Analog Devices. LTspice. URL https://www.analog.com/en/design-center/design-tools-and-calculators/ltspice-simulator.html.

[4] R. Gambotto. Analog front-ends for long range capacitive sensing for iot indoor human localization. *Supervisors: Luciano Lavagno, Mihai Teodor Lazarescu*, pages 222–229, 2017.

[5] T. Grosse-Puppendahl, C. Holz, G. Cohn, R. Wimmer, O. Bechtold, M. S. Hodges, S.and Reynolds, and J. R. Smith. Finding common ground: A survey of capacitive sensing in human-computer interaction. *Proceedings of the 2017 CHI Conference on Human Factors in Computing Systems, CHI '17, (New York, NY, USA)*, pages 3293–3315, 2017.

[6] J. Iqbal, M. T. Lazarescu, A. Arif, and L. Lavagno. High sensitivity, low noise front-end for long range capacitive sensors for tagless indoor human localization. *2017 IEEE 3rd International Forum on Research and Technologies for Society and Industry (RTSI)*, pages 1–6, Sep 2017.

[7] the free encyclopedia jjbeard on Wikipedia. Circuit diagram of a standard 555 astable circuit. URL https:// commons.wikimedia.org/wiki/File:555 Astable Diagram.svg, 2006.

[8] T. Kivimäki, T. Vuorela, P. Peltola, and J. Vanhala. A review on device-free passive indoor positioning methods. *International Journal of Smart Home*, 8(1):71–94, 2014.

[9] kuku Tena Nigatu. Tagless long/distance capacitive sensors for indoor human localizations. *Supervisors: Luciano Lavagno, Mihai Teodor Lazarescu*, 2018.

[10] Mihai Teodor Lazarescu. Drift Rejection Differential Frontend for Single-Plate Capacitive Sensors. *IEEE*, 2020.

[11] P. Poolad. Optimization of capacitive sensor front-end for indoor human localization and identication. *Supervisors: Luciano Lavagno, Mihai Teodor Lazarescu*, 2017.

[12] H. Prance, P. Watson, R. J. Prance, and S. T. Beardsmore-Rust. Position and movement sensing at metre standoff distances using ambient electric feld. *Measurement Science and Technology*, 23:115101, Oct 2012.

[13] H. Prance, P. Watson, R. J. Prance, and S. T. Beardsmore-Rust. A tagless indoor localization system based on capacitive sensing technology. *Sensors*, 16(9), 2016.

[14] J. Smith, T. White, C. Dodge, J. Paradiso, N. Gershenfeld, and D. Allport. Electric field sensing for graphical interfaces. *EEE Computer Graphics and Applications*, 18:54–60, May 2017.

[15] X. Tang, J. Liang, Y. Wang, and S. Mandal. Indoor occupancy awareness and localization using passive electric field sensing. *IEEE SENSORS*, pages 1–4, Oct 2018.

[16] M. Youssef, M. Mah, and A. Agrawala. Challenges: device-free passive localization for wireless environments. *Proceedings of the 13th annual ACM international conference on Mobile computing and networking*, pages 222–229, 2007.